

**UNCLASSIFIED**

---

---

**AD 277 363**

---

*Reproduced  
by the*

**ARMED SERVICES TECHNICAL INFORMATION AGENCY  
ARLINGTON HALL STATION  
ARLINGTON 12, VIRGINIA**



---

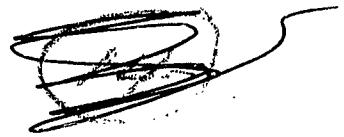
---

**UNCLASSIFIED**

NOTICE: When government or other drawings, specifications or other data are used for any purpose other than in connection with a definitely related government procurement operation, the U. S. Government thereby incurs no responsibility, nor any obligation whatsoever; and the fact that the Government may have formulated, furnished, or in any way supplied the said drawings, specifications, or other data is not to be regarded by implication or otherwise as in any manner licensing the holder or any other person or corporation, or conveying any rights or permission to manufacture, use or sell any patented invention that may in any way be related thereto.

2863

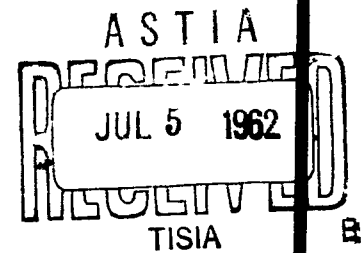
277 363



DASA - 1282

# MODEL FOR PREDICTION OF RETINAL BURNS (U)

1 FEBRUARY 1962



Headquarters  
DEFENSE ATOMIC SUPPORT AGENCY  
WASHINGTON 25, D.C.



by  
JOHN L. WRAY  
1st LIEUTENANT, USAF

TECHNICAL STAFF STUDY

DASA - 1282

MODEL FOR PREDICTION OF RETINAL BURNS

by

John L. Wray  
1st Lieutenant, USAF

SPECIAL PROJECTS BRANCH  
TEST PLANS AND PROGRAMS DIVISION  
DEPUTY CHIEF OF STAFF, WEAPONS EFFECTS AND TESTS

Defense Atomic Support Agency Technical Staff Studies are reports which have been prepared as preliminary working papers to present the current state of knowledge in a particular field. They are published solely to present to personnel interested in the same general field the current situation on the subject and to stimulate further thought and form a basis for further action. The author would appreciate comments or suggestions.

\* \* \* \* \*

1 February 1962

HEADQUARTERS, DEFENSE ATOMIC SUPPORT AGENCY  
WASHINGTON 25, D.C.

### ACKNOWLEDGEMENTS

Dr. W.T. Ham, Jr., Walter Geeroets, M.D., and other members of The Medical College of Virginia, Richmond, were particularly instrumental in pointing out the need for a physical computational method and in encouraging its development. Moreover, George Mixter, M.D., and Willard Derksen of the Naval Material Laboratory, Brooklyn, N.Y., were helpful in supplying the material on the damage integral.

Due credit should be given to Mr. B. L. Blackburn, Jr., DASA, who programmed the theory in FORTRAN II, and who devised the many necessary innovations necessary. Mr. Laurence S. Coşan, Operations Evaluation Group, USN, supplied the computer selection method for the relaxation procedure. SP-4 James R. Miller, DASA, prepared the final draft.

Although acknowledgement is made as to the contributions of the above individuals, the author assumes full responsibility for this report's contents.

ABSTRACT

A theory for a method of predicting chorioretinal burns from nuclear weapon explosions is presented. Description of a computer program in FORTRAN II for use on IBM 704, 709, or 7090 is given. The calculation results in spatial and time varying temperature profiles in the energy absorbing layers of the eye tissue. Applying tissue damage criteria to the results will allow analysis of estimates of danger and safe distances for viewing nuclear explosions.

TABLE OF CONTENTS

Title Page . . . . .	1
Acknowledgements . . . . .	ii
Abstract . . . . .	iii
Figures and Tables . . . . .	v
Theory on Retinal Burn Prediction . . . . .	1
Section I: Thermal Energy Production from the Fireball . . . . .	1
Section II: Atmospheric Transmission . . . . .	5
Method . . . . .	7
Horizontal Path . . . . .	8
Slant Path . . . . .	9
Section III: Energy Transmission and Absorption in the Eye, and Method of Calculating the Temperature Produced . . . . .	10
Absorption in P.E. (Region 1) . . . . .	10
Absorption in Choroid . . . . .	11
Initial and Boundary Conditions . . . . .	14
Grid Size . . . . .	17
Provision for other Attenuators . . . . .	19
Calculation of Henrique's Damage Integral . . . . .	19
Damage Criteria . . . . .	20
Results . . . . .	21
Operation Notes . . . . .	21
Appendix A . . . . .	22
Bibliography . . . . .	44
Distribution . . . . .	46

FIGURES

Figure 1. Schematic Diagram of Absorption and Conduction Volume	16
Figure 2. Relaxation Grid Numbered to Show Progression of Applying Equation (3.7)	16
Grid Size Figure	18

TABLES

Table A-1 Values of Precipitable Water Vapor for a Typical Pacific Atmosphere as Might be Found Near Hawaii in the Fall	22
Table 1 Normalized Time vs. Fireball Temperature and Radius	24
Table 2 Listing of Computer Program	25
Table 3 PTRAW, QTRAN, ABSMO	32
Table 4 Decimal Percent	33
Table 5 ABSI, ABSII	34
Table 6 Sample of Co. . . . . Run	35

## THEORY ON RETINAL BURN PREDICTIONS

Making predictions on the occurrence of retinal burns in persons or animals from a nuclear detonation essentially resolves itself into three separate, distinct problems. The first is the production of the thermal energy from the fireball itself; second is transmitting this energy through the intervening medium of atmosphere to the eye; and third is transferring this energy through the eye and depositing it in the layers of the eye in which heat and an accompanying temperature rise are produced due to the absorption of this energy. After considering each of these three areas separately, they are put together into one model which integrates the particular variables of each area. This model attempts to calculate the temperature rise in the retinal layers for a given explosion-observer relationship.

### SECTION I. THERMAL ENERGY PRODUCTION FROM THE FIREBALL

For the purposes of this study, it is assumed that the fireball radiates as a black body obeying Planck's law for the energy density of an isothermal black body (Ref. 23):

$$\psi_{\lambda} d\lambda = \frac{8\pi ch}{\lambda^5} \cdot \frac{1}{e^{(ch/\lambda kT_{fb})} - 1} d\lambda \text{ ergs/cm}^3 \quad (1.1)$$

$$E = 1/4cA\psi = \frac{cA}{4} \int_{\lambda_1}^{\lambda_2} \psi_{\lambda} d\lambda \quad \text{cals/cm}^2/\text{sec} \quad (1.2)$$

where:  $k = 1.380 \times 10^{-16}$  erg/°C (Boltzmann Constant)

$h = 6.625 \times 10^{-27}$  erg sec (Planck's Constant)

$\lambda$  = wavelength

$c = 3 \times 10^{10}$  cm/sec.

$T_{fb}$  = temperature of radiating body (in this case, the fireball)

$\Psi$  = energy density (ergs/cm<sup>3</sup>)

$E$  = total emissive power between  $\lambda_1$  and  $\lambda_2$  of  $\Psi$  (cals/cm<sup>2</sup>/sec)

$A = \frac{10^{-7}}{4.2}$  cals/erg

Equation 1.2 states the energy transfer across the surface maintained at temperature ( $T_{fb}$ ). It is seen, therefore, that in order to estimate the energy flux across the fireball surface as the explosion progresses in time, it is necessary to estimate the temperature at which the fireball is radiating from the time of explosion of the nuclear materials of the bomb to the time in which most of the energy is dissipated from the fireball. It should be recognized that the phenomena of fireball growth depends upon the type of atmosphere in which it is exploded: if the shot is exploded within the atmosphere the fireball behaves differently than an explosion in outer space. Table 1 gives the sets of values of temperatures, radii, and corresponding times after explosion for a typical 1 KT explosion in sea level air which have been used in this program. It is assumed that the intensity of the fireball (temperature) does not vary greatly with yield, and that the various phases (time development) of the fireball phenomena scale as the square root of the yield. Also given are the corresponding radii of the fireball for the given times. It is assumed that these radii scale with yield to the 0.4 power of the yield.

In the following paragraphs, reference should be made to Table 2 which lists the program of the model in Fortran II language and procedure.

These relationships were scaled from information in Chapters 2 and 7 of Reference 15. The range of time given therein is not for sufficiently short or long enough times; therefore, straight line extrapolation on log-log plot has been used to find the higher temperatures at shorter times, and straight line extrapolation was also used up to two seconds, after which a negligible temperature and a constant radius are used to fill out the times (for computational purposes). Because two seconds is more than  $60 t_{\max}$ , there will be less than 10% of the thermal energy remaining in the fireball, and its radiation rate will be very slow compared to earlier times.

It is necessary to calculate the energy release as a function of wavelength as well as time (through the temperature variation) because the atmosphere is wavelength selective as to transmissivity, as is also the pre-retinal ocular media. In addition, recent research results (Reference 1) have shown the energy absorption in the retinal layers to be wavelength dependant, so the energy must be carried through the entire model as a function of wavelength before being absorbed. As a practical matter, the wavelength range is limited to the range between 3500 and 15,000 Ångstroms, because of the ultra-violet cut-off in the atmosphere and the infra-red limitation in the spectral absorption of the pre-retinal ocular media. A wavelength band width of 100 Å is used.

There is no doubt that the interpretation of the fireball irradiance in this manner is grossly simplified, but because of the level of knowledge in the other areas and because of limitations of certain data, it is not deemed necessary to apply more sophisticated techniques until more complete information is assembled on tissue burn criteria, etc. However, modifications of the temperatures and radii used to better reflect actual situations would be well worthwhile in the prediction process when such information becomes available.

In the computation of the energy emission, the prediction program does it on a spectral basis for each of 115 wave bands of 100 Å width, beginning at 3500 Å.

$$I_{\lambda} = \frac{c T_{\lambda} E_{\lambda}}{(N_f)^2}$$

where:  $I_{\lambda}$  is irradiance on retina, uncorrected for pre-retinal ocular media scattering and absorption (cal/cm<sup>2</sup>/sec/cm) (FLL(I,J) in program).

$c$  is appropriate units conversion factor.

$T_{\lambda}$  is atmospheric transmission value.

$E_{\lambda}$  = fireball emissive power (cal/cm<sup>2</sup>/sec/cm)

$N_f$  = "f-number" of eye.

This information (the  $I_{\lambda}$  or FLL (K) values) together with the fireball radius, is stored on tape, after applying atmospheric corrections, for the particular time period under consideration. It should be noted that the program utilizing Sense Switch # 3, (Table 2), will allow energies to be read directly into the relaxation program, so that the method outlined above for computing energy is not a pre-requisite to using the program

to compute the tissue temperature rise. In order to know the energy per unit area falling on the lens of the eye and within the image on the retina (uncorrected for ocular scattering and absorption) the values of  $\Sigma MD$  and  $\Sigma M$  are calculated. These values represent the total energy per unit area delivered to 1) the most center point of the image and 2) upon the lens surface, respectively.

## SECTION II: ATMOSPHERIC TRANSMISSION

The amount of attenuation of radiant energy emitted from the fireball by the atmosphere depends upon the energy distribution (as a function of wavelength), the atmospheric composition, and the distance the observer is from the source. For the retinal burn problem, any energy which is either scattered or absorbed does not contribute to production of a temperature rise in the image area or the retina, unless the scattered radiation is multiply scattered in such a manner as to appear optically to originate in the fireball. Such multiple scattering is neglected in this model.

Degradation of the energy is mainly due to scattering of the dry air and scattering and absorption of the water vapor in the air. Quantitatively, the amount of scattering is dependant upon the number of scattering molecules (air density) while the amount of water vapor determines the scattering and absorption (temperature and relative humidity). Therefore, an atmosphere must be chosen and the density, temperature, and relative humidity specified quantitatively. The absorption coefficients of a standard atmosphere for each wavelength band must be corrected for the atmosphere chosen, then the total transmission coefficient for each wave band determined over the entire distance of the

path between fireball and the receiving eye (References 17 and 18).

In the part of the prediction model dealing with this calculation, two methods for calculating this transmissivity are used, both of which are based on a "flat earth" model. At large distances, a "flat earth" model will overestimate the transmission. Calculations of TRAN (L) or TRAN (M) (Table 3) depends upon whether there is an altitude difference between the source and receiver. If an altitude difference does exist, TRAN (L) is used: if there is not, TRAN (M) is calculated. The basic difference is that TRAN (L) allows for a variation in atmospheric density in the choice of constants and in the method of calculation (based on concept of "reduced height" atmosphere). These transmission coefficients are calculated for each of the 115 wavelength bands of 100 Å width and stored in memory to be used to calculate the energy emission spectrum (FLL(K)), described in Section I.

In dealing with the calculation of the atmospheric transmission, the situation that develops may be described as being "extremely precise and highly inaccurate". An intricate calculation method has been developed and is presented for use. However, because of the limited accuracy of the input data and because of the fallacy of trying to estimate temperature, relative humidity, and atmospheric composition under an average situation, the power of the method is limited to the accuracy of the known and specified conditions. Indeed, here is one area where a general method cannot overcome lack of specific data and facts.

The following paragraphs will outline the method developed and data

will be given, such as it is, for a typical Pacific Ocean atmosphere on a typical winter day at a typical time. It should be stressed that lack of experience with the program precludes a knowledgeable evaluation of the effect of various changes in the atmospheric input, but it is felt that unless appreciable range of values for a specific location or situation exist, the atmospheric transmission may be regarded as a second order effect in view of the highly influential uncertainties in the other areas, such as weapon radiation output and tissue temperature damage criteria.

#### Method

The method used to estimate the atmospheric transmission is that outlined on page 432 of Reference 18. The method is based on observations of the transmission of solar radiation through a cloudless atmosphere (assumed dust free):

$$a_{\lambda} = a_{a\lambda} (a_{w\lambda})^w$$

where:  $a_{\lambda}$  is the spectral transmission coefficient for a vertical path (optical air mass unity, when  $p=p_0$ ).

$a_{a\lambda}$  is the vertical transmission considering only the effect of scattering by pure dry air.

$a_{w\lambda}$  is the transmission considering only the effect of scattering by 1 cm of precipitable water vapor.

$w$  is the amount of precipitable water in the path, measured in cm.

For this study the relationship was modified to account for any straight path:

$$a_{t\lambda} = (a_{a\lambda})^m (a_{w\lambda})^{wm}$$

where:  $a_{t\lambda}$  is the total transmission factor for any chosen optical path.  
 $m$  is the number of air masses in the optical path.  
 $w \cdot m$  is the total precipitable water vapor in the chosen optical path.

Table 3 gives values of  $a_{a\lambda}$  and  $a_{w\lambda}$  (called PTRAN and QTRAN in the program) based on Reference 18, pages 431, f.f.

The Smithsonian tables also recognize absorption by the water vapor in the air and present corrections for this based on a spectrally integrated transmission coefficient. This correction is not applied to this problem for the following reasons:

1. It is not given spectrally.
2. The largest effect of the water vapor absorption would be in the lower and upper wavelength regions of the spectrum considered in this study. Because these regions are highly affected by the atmospheric scattering and the pre-retinal ocular absorption and scattering, its total effect on the total energy transmitted would be almost negligible, when these other attenuations are considered and accounted.

To account for both horizontal and slant paths, two relationships for  $a_{t\lambda}$  are used:

Horizontal path

$$a_{t\lambda} = (a_{a\lambda})^s (a_{w\lambda})^{w \cdot m}$$

where:  $s$  = horizontal distance in miles divided by 5.25 miles which is the distance through an amount of sea level atmosphere equivalent to a vertical path (optical air mass unity, when  $p = p_0$ ).

This is written in the program as:

$$\text{TRAN}(M) = \left[ \text{PTRAN}(M) \right]^s \left[ \text{QTRAN}(M) \right]^{\text{CON} : 5}$$

8

Slant path

$$a_{t\lambda} = \left\{ \left[ 1.0 - (M_L - M_H) (1.0 - a_{a\lambda}) \right]^A \right\} (a_{w\lambda})^{C W_{MF} D H_T}$$

where:  $M_L$  is the vertical air mass decimal percent above the lower altitude (of observer or explosion). See Table 4.

$M_H$  is the vertical air mass decimal percent above the higher altitude (of observer or explosion). See Table 4.

The above equation has been written in the program as:

$$\text{TRAN(L)} = (1.0 - \text{CON } 4(1.0 - \text{PTRAN(L)}))^A (\text{QTRAN(L)})^{\text{CON } 3}$$

where:  $A = \left[ 1 + \left( \frac{D}{h} \right)^2 \right]^{1/2}$

D is the horizontal distance.

h is the vertical distance between explosion and observer.

$C \cdot W_{MF} \cdot H_T$  represents the average precipitable water vapor over the slant distance per horizontal mile of optical path (measured in centimeters of water).

$W_{MF}$  is the water vapor multiplication factor which accounts for the assumption that there is negligible water vapor above a level of 5 miles altitude above sea level and that the lower of the observer or explosion altitude may or may not be at sea level.

For calculation of this factor, see Appendix A.

C is a constant which represents the centimeters of precipitable water vapor per horizontal mile of air at sea level. For Pacific atmosphere at 25° C and 100% relative humidity, an approximation for C at sea level is 3.48 cm. (See Table in Appendix A for

other values of C, as a function of altitude. If the type of atmosphere is changed, other values of C for the new location will be needed.)

$H_r$  is the relative humidity averaged with water content over the optical path.

D is the horizontal distance between observer and explosion.

SECTION III: ENERGY TRANSMISSION AND ABSORPTION IN THE EYE, AND METHOD OF CALCULATING THE TEMPERATURE PRODUCED

(The calculation of a temperature rise in the retinal layers)

Research results (Reference 1) have yielded values which may be used as energy transmission values (as a function of wavelength) through the pre-retinal ocular media. These are presented as a function of the 115 wavelength bands of 100 Å each in Table 3. Table 5 presents the total absorption coefficients (in decimal percent) used for the layers of pigmented epithelium and the choroid, as a function of wave length for 100 Å bandwidths, starting at 3500 Å (Reference 1). These three factors are appropriately applied to determine the absorption in each of the two layers. (Refer to Figure 1: 1 denotes region of P.E., 2 denotes region of choroid, and 3 denotes the volume surrounding regions 1 and 2).

Absorption in P.E. (Region 1) -- cal/cm<sup>3</sup>/sec

$$AI = \sum_{\lambda = 3,500 \text{ Å}}^{15,000 \text{ Å}} \frac{FLL(\lambda)}{RET} (1-ABS_{MO}(\lambda)) (ABS_I(\lambda)) \Delta \lambda \quad (3.1)$$

where: RET is thickness of P.E. ( $\approx 10\mu$ ).

$\Delta \lambda = 100 \text{ Å}$ .

Absorption in Choroid (Region 1) -- cal/cm<sup>3</sup>/sec

$$A_{II} = \sum_{\lambda = 3500 \text{ \AA}}^{15,000 \text{ \AA}} \frac{F_{LL}(\lambda)}{R_{RET}} (1 - ABS_{MO}(\lambda)) (1 - ABS_I(\lambda)) (ABS_{II}(\lambda)) \Delta \lambda \quad (3.2)$$

where CHOR is the thickness of choroid (for humans  $\approx 80\mu$  to  $100\mu$ ).

A correction factor of  $\frac{R^2}{(3.5 \times 10^{-4})}$  is applied to AI and AII if the radius of the image (R in centimeters) is less than  $3.5\mu$ , which is considered to be an average image limitation value, based on chromatic aberration, diffraction, and corrected for a  $\frac{1}{\lambda^4}$  energy distribution (Reference 19).

The resulting values of AI and AII are then used as heat sources in a heat conduction problem which attempts to calculate the spatial and time varying temperature profiles in the volume, including, and surrounding the volume defined by the fireball optical image on the retina and the layer thickness of the absorbing tissues.

Certain basis assumptions are made about the "heat generation" model. It is assumed that all tissue thermal properties are nearly the same as water and that absorption and conduction occur uniformly. No corrections are made for changes in tissue temperature. All heat that is not absorbed in the pigmented epithelium or choroid is discarded as not causing a significant contribution to the temperature rise in those two regions. There is assumed conduction in the tissue surrounding the absorbing volume, but no heat generation. The absorbing volumes "grow" in radius as the image radius expands with time as a result of fireball growth, but the thicknesses of absorbing properties do not vary with time or change with temperature. Re-radiation of energy due to the local temperature rise in the area of the absorbing volume is neglected. There is some indication (Reference 20) that the absorbing of the radiant

energy in the pigmented epithelium does not take place uniformly, but is absorbed in pigmented cells which are interspaced between semi-transparent tissue. This local absorption effect is neglected in the model, as quantitative information on this method of absorption is not available. However, the surface to volume ratio of these cells is considered to be so large that there should not be appreciable build-up in temperature within them before conduction will dissipate the heat to the surrounding tissues. Should the heat generation perform more as surface heating than volume heating in these cells, an entirely different method of treating the heat source would be required. However, this remains to be proven experimentally or otherwise demonstrated formally.

The fundamental heat conduction equation is (Reference 21):

$$\nabla^2 v(t) + \frac{A(i)}{k} = \frac{\rho c_p}{k} \frac{\partial v(t)}{\partial t} \quad (3.3)$$

where:  $k$  = conductivity of material.

$\rho$  = density of material.

$c_p$  = specific heat of material.

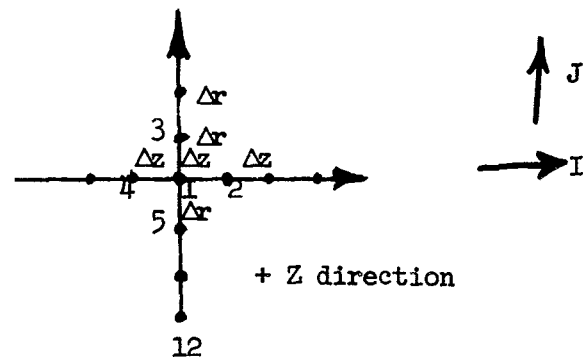
$\nabla^2$  = Laplacian operator.

$v(t)$  = temperature as a function of time.

$t$  = time.

$A(i)$  = volume absorption rate in region (i).

Equation 3.3 is put into difference equation form according to the following diagram:



Expressing the Laplacian operator in terms of a cylindrical difference equation for the temperature of point 1 in terms of points adjacent to points 3, 5, 6, and 9 yields:

$$\nabla^2 v = \frac{\partial^2 v}{\partial r^2} + \frac{1}{r} \frac{\partial v}{\partial r} + \frac{\partial^2 v}{\partial z^2} \quad \text{for } \frac{\partial v}{\partial \phi} = 0$$

$$\frac{\partial^2 v}{\partial r^2} \approx \frac{v_3 - v_1}{\Delta r} - \frac{v_1 - v_5}{\Delta r} = \frac{v_5 - 2v_1 + v_3}{\Delta r^2}$$

$$\frac{\partial^2 v}{\partial z^2} \approx \frac{v_2 - v_1}{\Delta z} - \frac{v_1 - v_4}{\Delta z} = \frac{v_4 - 2v_1 + v_2}{\Delta z^2}$$

$$\frac{\partial v}{\partial r} \approx \frac{v_3 - v_5}{2\Delta r}$$

$$\therefore \nabla^2 v \approx \frac{v_5 - 2v_1 + v_3}{\Delta r^2} + \frac{v_3 - v_5}{2r\Delta r} + \frac{v_4 - 2v_1 + v_2}{\Delta z^2} \quad (3.4)$$

$$P1 = \frac{A(1)}{k} = \frac{AI}{k} \quad (\text{for region 1}), \quad (3.5)$$

$$P1 = \frac{A(2)}{k} = \frac{AII}{k} \quad (\text{for region 2}), \quad (3.5)$$

$$P1 = \frac{A(3)}{k} = 0 \quad (\text{for region 3}) \quad (3.5)$$

$$\frac{\partial v}{\partial t} \approx \frac{v_1 - v_{1(n-1)}}{t - t_{(n-1)}}, \quad (3.6)$$

where: subscript n-1 refers to the temperature at point 1 at the preceding relaxation time.

Equation 3.4, 3.5, and 3.6 then are used to approximate Equation 3.3 in finite difference form:

$$\frac{v_5 - 2v_1 + v_3}{\Delta r^2} + \frac{v_3 - v_5}{2r\Delta r} + \frac{v_4 - 2v_1 + v_2}{\Delta z^2} + P1 = \left( \frac{\rho c_p}{k} \right) \frac{v_1 - v_{1(n-1)}}{t - t(n-1)}$$

from which :

$$v_1 = \frac{\frac{v_5 + v_3}{\Delta r^2} + \frac{v_3 - v_5}{2r\Delta r} + \frac{v_4 + v_2}{\Delta z^2} + P1 + \frac{\rho c_p}{k} \frac{v_1 (n-1)}{t - t(n-1)}}{\left( \frac{\rho c_p}{k(t_1 - t(n-1))} + \frac{2}{\Delta r^2} + \frac{2}{\Delta z^2} \right)} \quad (3.7)$$

#### Initial and boundary conditions

At  $t = 0$ , all grid points  $v(I,J) = 0$ ,

where:  $1 \leq J \leq \text{LAT}$ ,  $1 \leq I \leq \text{LONG}$ , I and J integers, LAT and LONG

defining the number of grid points in the radial and axial directions.

Equation 3.7, therefore, calculates the temperature rise above the ambient body temperature, which may be chosen to reflect the body temperature of subject being considered. (However,  $v(I,J) = T$  where T is any value, by changing statement  $T = 0.0$  following statement 11 of the program; calculated temperatures would then be actual temperatures if T were body temperature.)

Absorption function P1 is defined by equations (3.5).

At the boundaries between regions 1 and 2, 1 and 3, and 2 and 3,

$$v_1 = v_2, v_1 = v_3 \text{ and } v_2 = v_3.$$

$$\text{Also: } \frac{\partial v_1}{\partial z} = \frac{\partial v_2}{\partial z}$$

$$\frac{\partial v_1}{\partial r} = \frac{\partial v_3}{\partial r}, \quad \frac{\partial v_1}{\partial z} = \frac{\partial v_3}{\partial z}$$

at the appropriate boundaries.

$$\frac{\partial v_2}{\partial r} = \frac{\partial v_3}{\partial r}, \quad \frac{\partial v_2}{\partial z} = \frac{\partial v_3}{\partial z}$$

In region 3, the outer cylindrical boundary is assumed to be non-conductive so that:

$$\frac{\partial v_3}{\partial r} = \frac{\partial v_3}{\partial z} = 0$$

at outer grid points.

To effect this condition,

$$v(1,J) = v(2,J)$$

$$v(I,25) = v(I,24)$$

$$v(49,J) = v(48,J)$$

(Numbers 24, 25, 48, 49 would depend upon grid size -- these are LAT - 1, LAT, LONG - 1, and LONG, respectively.)

is dictated by the program. The physical effect of this is that no heat is lost from region 3. As long as region 3 is kept large compared to regions 1 and 2, it is felt that no loss of heat from region 3 counter-balances neglecting absorption in region 3. Heat generation in the three regions is governed by equation 3.5 stated previously.

From the above, it is seen that the temperature of any point in a grid can be found if the heat source, the previous temperature of that point, and the surrounding four temperatures are known. A grid is set up in the retinal layers to represent a radial plane of a right circular cylinder.

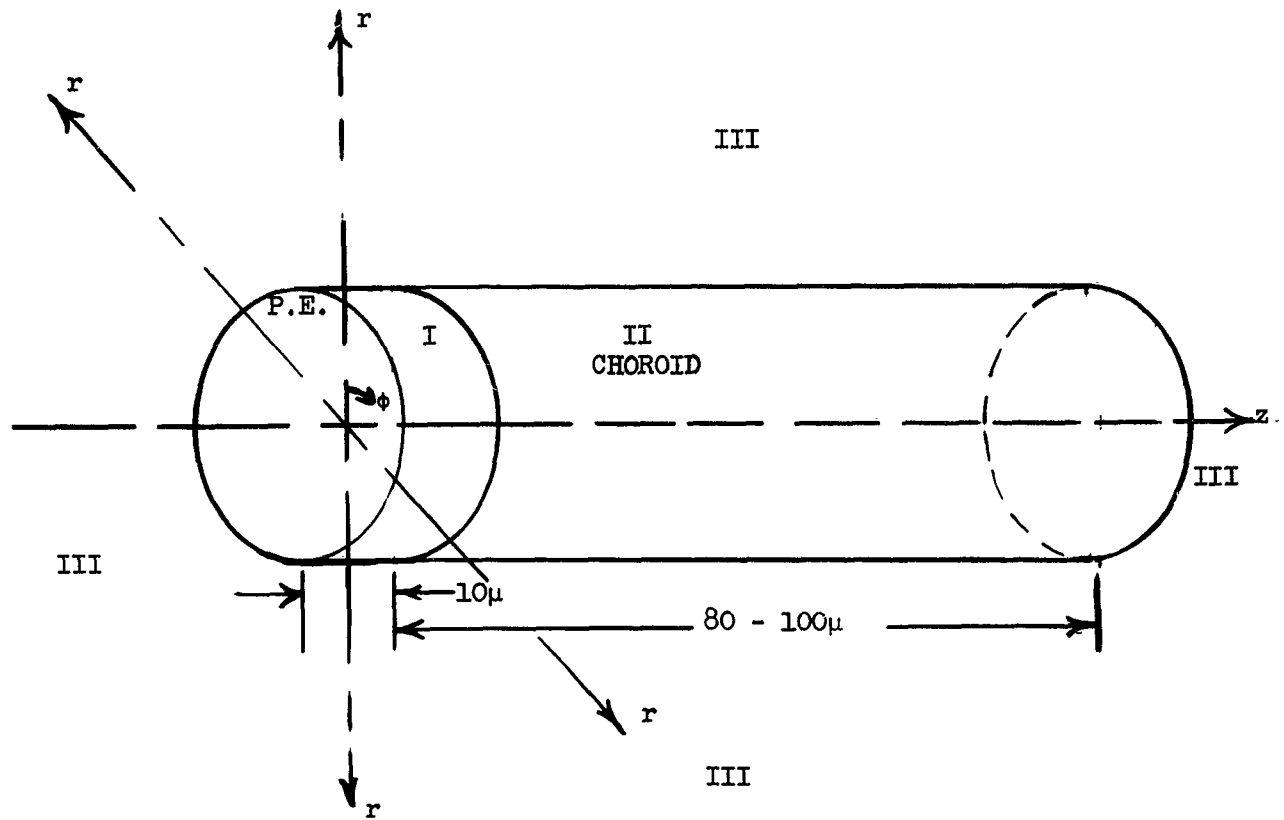


Figure 1. Schematic Diagram of Absorption and Conduction Volume

It is assumed that the energy absorption (and hence the temperatures) does not vary with angle  $\phi$ .

The resulting grid is as follows (numbers refer to sequence of applying equation (3.7)).

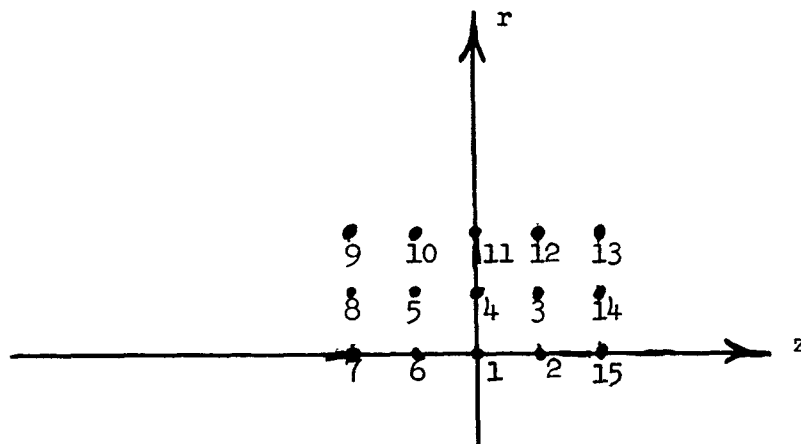


Figure 2. Relaxation Grid Numbered to Show Progression of Applying Equation (3.7).

Equation 3.7 is applied first at point 1, then at point 2, etc., in a hemispherical motion about a center of point 1. By progressing in this manner through the grid several times, the temperature of each grid point "relaxes" to values which approximate the temperatures for the time specified. A test is built into the program so that when the largest change in temperature of any point in the grid is less than a pre-assigned percentage of the largest temperature in the grid, the relaxation procedure is halted. The smaller this TEST percentage is made, the greater the accuracy of the results. Experimentation with this value is needed in most situations. The grid in Figure 2 is superimposed on Figure 1 so that the starting point (point 1) is the center of the pigmented epithelium layer, on the z axis. The size of the grid is chosen to be about 3 times the largest image radius and about three or four times as long as the thickness of the choroid.

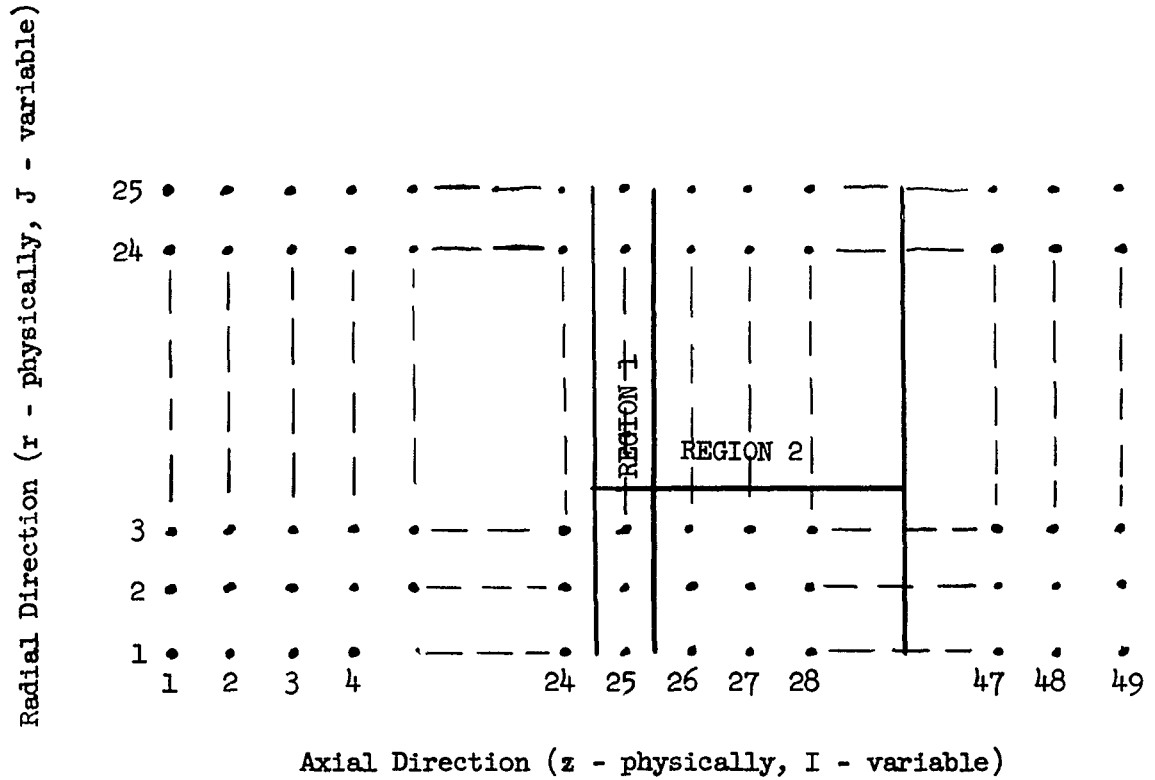
After a relaxation is completed for one time period, time is incremented and new  $A_{(j)}$  values are calculated and the relaxation process commenced again. The program halts or goes to the next program when zeroes appear in FTIMS(I) and DELTI(I). (Therefore, FTIMS(9) and DELTI(9) must always be zero.)

Typical variable data input is listed in Table 6. Results of the calculations for the temperature profiles at various stages of the explosion development are listed in Table 6.

#### Grid size

The grid used presently for this program is 49 points in the z (axial) direction and 25 points in the r (radial) direction (a point is denoted by (I,J) variables as to point location, i.e., (25,1) denotes

center of pigmented epithelium on z axis, (4,13) denotes the 4th radial point from the center line which is in z column number 13.



The physical side of the grid depends upon the values for  $\Delta r$  and  $\Delta z$ . These values are usually selected by estimating the largest image radius, multiplying this value by 3 to allow for conduction, and then dividing it by the number of radial space increments.

$$\Delta r = \frac{3r_1 \text{ (largest)}}{24} = \frac{r_1 \text{ (largest)}}{8}$$

It is generally convenient to let  $\Delta z = \Delta r$ , but the product of  $\Delta z$  and the number of axial grid points must generally be at least 300 to 400

microns in order to allow proper conduction axially.

#### Provisions for other attenuators

A Constant Attenuation Factor (abbreviated CAF in the program) is provided so that attenuators such as plexiglass or fixed, constant density (with wavelength) filters may be accommodated. The proper transmission value of the attenuator (in decimal percent) is then stated in the input variable for CAF. If no such attenuator is present in the physical problem, a value of CAF = 1.0 is inserted as the value for CAF. (Actually, the words "constant attenuation factor" are a misnomer -- it should be "constant transmission factor" because of its method of use.)

#### Calculation of Henriques' Damage Integral

There is a provision in the program (c.f. statements 150 to 154) for calculating the integrated cellular damage based on the Henriques' Damage Integral empirical relationship. This calculation can be utilized by placing Sense Switch 4 in the down position. The calculation for  $\Omega$  is made for various grid points which are determined by reading, as input, various values of LEX(I); a pair of LEX(I) values corresponding to a grid point in terms of (I,J). By changing the statement following statement 400 ( $\Sigma(L) = \text{etc.}$ ) any relationship for Henriques' function may be utilized. It is anticipated that this portion of the program may become increasingly valuable in applying damage criteria as the program is utilized in analyzing laboratory produced permanent damage where the damage producing temperature may be estimated by staining technique. Ultimately, however, the dependance will be directly related to the confidence in the Henriques' relationship used.

### Damage criteria

In order for this model to be effective, some criteria must be established to determine when irreparable damage occurs. Previous attempts (References 22 and 16) have been to specify the damage thresholds in terms of irradiance (cals/cm<sup>2</sup>/sec) radiant exposure (cals/cm<sup>2</sup>), image size, and time of exposure. It is now thought that the temperature of the absorbing and conducting tissue of the retina is more fundamental to the damage mechanism than the total energy or energy rate of deposition. If this be true, the damage criteria should be related to the temperature-time history of the irradiated material. Research efforts (at the Medical College of Virginia) are now in progress to attempt to demonstrate this point. If this damage relationship can be found experimentally, it would provide damage criteria for the predictions produced by this program.

Until the laboratory results are available, an interim method to estimate the burn-damage criteria has been used to evaluate the results of calculations based on this model. It is reasoned that irreparable damage occurs where the tissue is heated above the temperature at which boiling of the fluids will occur ( ~ 100° C or a temperature rise of ~ 65° C). It is also thought that irreparable damage can occur when there is no evidence of boiling or vapor eruption in the tissue, which means a macroscopic maximum temperature somewhat below 100° C was obtained. On the lower end of the scale, it is thought that irreparable damage is not likely if a temperature rise of less than 20° C exists for a short time (less than a second).

Thus, it is reasoned that a temperature rise of greater than 20° C, but less than 65° C, for a time period of the order of the blink reflex

or less, will be the temperature range in which irreparable damage is produced. A more specific criteria awaits further research results.

#### Results

Input values and results and print-out for a typical computer run are included in Table 6.

#### Operation Notes

This program has been operated on IBM 704, 709, and 7090 computers with 32,000 word memory units. Running time for an average problem is approximately 20 - 30 minutes on the 704 and 5 - 10 minutes on the 7090. A calculation using one yield and five distances to determine a safe distance requires about 35 minutes. Of course these times are highly dependant on the grid size, time increments, and TEST values used. Use of Sense Switch # 2 allows consecutive runs to be made without stopping the computer; however, the same input data must be used, and only the variable cards can be changed from run to run in this procedure. Computer units with 8k memories may be used by utilizing a smaller number of grid points.

APPENDIX A

Calculation of  $W_{mf}$  (WMFI)

Calculation of the precipitable water vapor multiplication factor may be demonstrated from the following:

TABLE A-1

Values of Precipitable Water Vapor for a Typical Pacific Atmosphere as Might be Found Near Hawaii in the Fall

Altitude (mi)	Temp (°C)	Water Vapor Density	Relative Humidity	Cm. of Precipitable Water Vapor per Horizontal Mile (100% Rel. Humidity) Constant C	Cm of Precipitable Water Vapor per Horizontal Mile at Indicated Relative Humidity
0.0	25	0.02178	0.80	3.48	2.78
0.5	17	0.01447	0.85	2.32	1.98
1.0	13	0.01135	0.80	1.82	1.46
1.5	10	0.00941	0.55	1.51	0.83
2.0	7.5	0.00800	0.42	1.28	0.54
2.5	4	0.00636	0.42	1.00	0.42
3.0	0.0	0.00485	0.42	0.78	0.33
3.5	- 6	0.00350	0.42	0.56	0.24
4.0	-13	0.00250	0.42	0.40	0.17
4.5	-23	0.00170	0.42	0.27	0.11
5.0	-34	0.00120	0.42	0.19	<u>0.08</u> 8.94

$$\text{Average from 0 to 5 miles} = \frac{8.94 - 0.08}{10} = 0.886 \text{ cm water/mile.}$$

$$\therefore C \cdot W_{mf} \cdot H_r = 0.886 \quad (\text{A.1})$$

$$W_{mf} = \frac{0.886}{C \cdot H_r} \quad (\text{A.2})$$

for values of  $C = 3.48$  and  $H_r = 0.5$ ,

$$W_{mf} = \frac{0.886}{3.48 \times 0.8} = 0.32 \quad (\text{A-3})$$

This is the value for  $W_{mf}$  for a slant path between altitudes of 0 and 5 miles, and an average relative humidity of 80% in the first several thousand feet of atmosphere.

Should the higher altitude be above 5 miles, a correction factor must be applied to  $W_{mf}$  to account for the fact that the entire horizontal distance (D) does not apply:

$$W_{mf} = \frac{0.886}{C \cdot H_r} \left( \frac{5}{h} \right) \quad (\text{A.4})$$

If the lower altitude is above sea level, the proportion of the last column in Table A-1 should be omitted in computing the average precipitable water vapor. For example, should the lower altitude be 3000' and the higher altitude 5 miles, the average precipitable water vapor would be  $\frac{8.86 - 2.78}{9} = 0.67$  cm water/mile. Therefore, equation A.1

should now be:

$$C \cdot W_{mf} \cdot H_r = 0.67 \quad (\text{A.5})$$

TABLE 1

Normalized time vs. fireball temperature and radius. (XNORT x 10<sup>8</sup> seconds --  
 TEMP1 x 10<sup>-3</sup> degrees C -- RADII x 10 feet).

00000010	00000020	00000030	00000040	00000050	00000060	00000070
20000	10000	9000	8200	7600	7000	6600
12	15	16	19	22	24	26
00000080	00000090	00000100	00000200	00000300	00000400	00000500
6400	5800	5600	3700	2800	2000	1700
27	29	30	42	49	59	65
00000600	00000700	00000800	00000900	00001000	00002000	00003000
1300	1100	920	800	740	340	210
69	75	80	87	89	120	140
00004000	00005000	00006000	00007000	00008000	00009000	00010000
150	120	92	80	62	60	54
170	190	200	220	240	250	260
00020000	00030000	00040000	00050000	00060000	00070000	00080000
23	15	11	9.0	7.4	6.4	5.5
300	430	480	530	560	580	620
00090000	00100000	00200000	00300000	00400000	00500000	00600000
4.8	4.4	2.2	1.8	1.9	2.2	2.5
660	680	880	990	1080	1140	1210
00700000	00800000	00900000	01000000	02000000	03000000	04000000
2.7	3.2	3.5	3.8	6.6	8.0	8.5
1260	1320	1350	1360	1680	1860	1960
05000000	06000000	07000000	08000000	09000000	10000000	20000000
8.5	8.2	7.8	7.0	6.4	5.9	3.4
1990	2040	2080	2100	2160	2190	2280
30000000	40000000	50000000	60000000	70000000	80000000	90000000
2.6	2.1	1.8	1.5	1.4	1.3	1.2
2340	2370	2410	2410	2410	2410	2410
100000000	200000000	300000000	400000000	500000000	600000000	700000000
1.1	0.7	0.7	0.7	0.7	0.7	0.7
2440	2470	2470	2470	2470	2470	2470
800000000	900000000	1000000000	1100000000	1200000000	1300000000	1400000000
0.7	0.7	0.7	0.7	0.7	0.7	0.7
2470	2470	2470	2470	2470	2470	2470
1500000000	1600000000	1700000000	1800000000	1900000000	2000000000	3000000000
0.7	0.7	0.7	0.7	0.7	0.7	0.7
2470	2470	2470	2470	2470	2470	2470
4000000000	5000000000	6000000000				
0.7	0.7	0.7				
2470	2470	2470				

TABLE 2

* PAUSE
*MAIN PROGRAM
* CARDS ROW
* LIBE
* LISTB

EYE PROBLEM PROGRAMED BY LAWTON BLACKBURN JR.

```
DIMENSION RUNNO(3),CLASSE(3)
DIMENSION RADI( 500),TEMP(500),BLK(49,25),BLK1(49,25),PTRAN(116),
1 FLL(116),QTRAN(116),XNORTI(90),TEMP1(90),RADII(90),ABSMO(116),ARSI
2 (116),ARSI1(116),DELTI(9),FTIMS(9),LEX(22),OMEGA(10),SIGMA(10),TRA
3 N(116)
IPAGE = 1
READ 174,(PTRAN(I),I=1,116)
READ 174,(QTRAN(I),I=1,116)
READ 174,(XNORTI(I),I=1,88)
READ 178,(TEMP1(I),I=1,88)
READ 180,(RADII(I),I=1,88)
READ 182,(ABSMO(I),I=1,116)
READ 182,(ARSI(I),I=1,116)
READ 182,(ARSI1(I),I=1,116)
9 READ 300,((RUNNO(I),I=1,3),(CLASSE(I),I=1,3))
READ 186,RET,CHOR,TEST,DEL7,DEIR,NO1,IM,IN,KK,LONG,LAT
10 READ 188,YIELD,ALT,DIST,FNUMR,ANGLE,FOCAL,AMUL,AMFL,AMFH,RELHI,CAF
1,WMPI
READ187,CON,CON2
IF(SENSE SWITCH 4)14,11
14 READ 175,(LEX(I),I=1,20)
DO 15 L = 1,10
15 OMEGA(L) = 0.0
11 READ 189,(DELTI(I),I=1,9)
READ189,(FTIMS(I),I=1,9)
SENSE LIGHT 1
X=0.0
T=0.0
LEX(21) = 0
LEX(22) = 0
K0=1
GO TO 413
12 FTIME = FTIMS(K0)
DELT = DELTI(K0)
NIDT=FTIME/DELT
13 TMAX=(.032*YIELD**2)
IF(YIELD-10.)16,17,17
16 TMAX=TMAX*1.3
17 J=1
DO 25 K=1,NIDT
X=X+DELT
Y=X/TMAX
22 IF(Y-XNORTI(J))24,24,23
23 J=J+1
GO TO 22
24 TEMP(K)=TEMP1(J)
25 RADI(K)=RADII(J)*YIELD**2
DWAVE=1.0E-6
CON3=CON*WMP1*DIST*RELHI
CON4=AMFL-AMFH
CON5=CON2*DIST*RELHI
IF(SENSE SWITCH 3)213,27
27 IF(ALT)208,32,28
28 A=(1.+(DIST/ALT)**2)**2
DO 30 L=1,116
```

EYE PROBLEM PROGRAMED BY LAWTON BLACKBURN JR.

```
30 TRAN(L)=((1.0-CON4*(1.0-PTRAN(L))**A)*(QTRAN(L)**CON3)
GO TO 35
32 S=DIST*AMFL/5.25
DO 34 M=1,116
34 TRAN(M)=(PTRAN(M)**S)*(QTRAN(M)**CON5)
35 REWIND R
Y1=COSE(ANGLE)
Z1=.224E-12
X1=1.44 E-3
40 DO 47 N=1,NIDT
41 BC=35.E-6
DO 46 JI=1,116
FL=Z1*TRAN(JI)/(BC**5*(2.71828**(X1/(BC*TEMP(N)))-1.))
FLL(JI)=FL*Y1/FNUMB**2
BC=RC+D*AVE
46 SUM=SUM+FLL(JI)*DWAVE*DELT
SUMD=SUM*FNUMB**2*RADI(N)**2/(5280.0**2)/(ALT**2+DIST**2)
47 WRITE OUTPUT TAPE 8,100,(FLL(K),K=1,116)
IF(K0-1)411,410,411
410 PRINT 301,(RUNNO(I),I=1,3)
PRINT 302
411 PRINT 303,SUM,SUMD,FTIME
202 LATA = LAT-1
203 LONGA = LONG-1
213 MID=(LONG+1)/2
214 TS=MID
50 N1=(RET/2.)/DELZ+TS
N2=(RET/2.+CHOR)/DELZ+TS
N3=TS-(RET/2.)/DELZ
C1=1./(2./DELZ**2+2./DELR**2+1./1.4E-3/DELT)
REWIND R
NO=NO1
IF(SENSE LIGHT 1)57,63
57 DO 62 I=1, LONG
DO 62 J=1, LAT
61 BLK(I,J)=I
62 BLK1(I,J)=I
63 DO 76 K=1,NIDT
READ INPUT TAPE 8,190,(FLL(I),I=1,116)
AI=0.0
AII=AI
DO 71 J=1,116
A1=FLL(J)*DWAVE/RET*(1.-ARSMO(J))*ABSI(J)
AI=AI+A1
A2=FLL(J)*DWAVE/CHOR*(1.-ARSMO(J))*(1.-ABSI(J))*ABSII(J)
71 AII=AII+A2
R=FOCAL*RADI(K)*AMUL/(DIST**2+ALT**2)**.5/5280.
IF(R-3.5E-4)72,73,73
72 AI=AI*(R/3.5E-4)**2
AII=AII*(R/3.5E-4)**2
73 T=T+DELT
L1=1.+R/DELR
79 I=MID
BIG=0.0
J=2
IJ=MID
```

## EYE PROBLEM PROGRAMED BY LAWTON BLACKBURN JR.

```

      JI=3
03  IF(I-IJ)89,84,89
04  IF(J-1)86,85,86
05  IF(I-(MID-1))96,96,92
06  IF(J-JI)104,87,87
07  IF(I-J-(MID-1))88,96,88
08  IF(I+J-(MID+1))100,92,100
09  IF(J-1)90,100,90
10  IF(I-J-(MID-1))108,104,108
11  IF(I-IJ)96,92,92
12  IJ=I
      JI=J
      I=I+1
      GO TO 114
06  IJ=I
      JI=J
      I=I-1
      GO TO 114
100 IJ=I
      JI=J
      J=J+1
      GO TO 114
104 IJ=I
      JI=J
      J=J-1
      GO TO 114
108 IF(I+J-(MID+1))91,104,91
114 IF(J-L1)115,115,123
115 IF(I-N2)116,121,123
116 IF(I-N1)117,119,121
117 IF(I-N3)123,119,119
119 P1=CAF*AI/1.4E-3
      GO TO 1124
121 P1=CAF*AI/1.4E-3
      GO TO 1124
123 P1=0.0
1124 IF(SENSE SWITCH 5)1125,124
1125 PRINT 1126,AI,AII,P1
1126 FORMAT(3E12.4)
124 IF(J-1)129,129,132
129 V3=RLK(I,J+1)
      V5=V3
130 S=10.
      GO TO 134
132 V5=RLK(I,J-1)
      V3=RLK(I,J+1)
133 AA=J-1
      S=AA*DELR
134 BK0=C1*((RLK(I-1,J)+BK(I+1,I))/DELZ**2+(V5+V3)/DELR**2-(V5-V3)/2.
      I/S/DELR+RLK(I,J)/1.4E-3/DELT+P1)
      DJD=B K0-RLK(I,J)
      IF(ABSF(DID)-BIG)139,139,138
138 BIG=ABSF(DID)
139 BLK(I,J)=B K0
140 IF(I-2)83,141,83
141 IF(J-1)83,142,83

```

```

142 DO143NN=1,LATA
143 BLK(1,NN)=BLK(2,NN)
DO145NN=2,LONGA
145 BLK(NN,LAT)=BLK(NN,LAT-1)
DO147NN=1,LATA
147 BLK(LONG,NN)=BLK(LONG-1,NN)
IF(SENSE SWITCH1)217,149
149 IF(HIG-TEST*BLK(MID,1))218,218,79
151 DO 153 NN=1, LONG
DO 153 NM=1, LAT
153 BLK1(NN,NM)=BLK(NN,NM)
IF(SENSE SWITCH 4)150,154
150 I = LEX(1)
J = LEX(2)
L = 0
400 L = L+1
SIGMA(L) = EXPF(137.8712-46650.0/309.+BLK(I,J)+LOGF(DELT))
OMEGA(L) = OMEGA(L)+STIGMA(L)
I = LEX(2*L+1)
152 J = LEX(2*L+2)
IF(I-0)400,154,400
154 IF(NO-NO1)155,158,155
155 NO=NO+1
156 CONTINUE
END FILE 6
END FILE 7
END FILE 8
KO =KO+1
IF(DELT I(KO))208,171,12
158 COUNT = 0.0
WRITE OUTPUT TAPE 6,304,((RUNNO(I),I=1,3),(CLASSF(I),I=1,3)),IPAGE
IPAGE = IPAGE + 1
COUNT = COUNT + 1.0
WRITE OUTPUT TAPE 6,104,T,R
COUNT = COUNT + 1.0
KN = IM
414 WRITE OUTPUT TAPE 6,106,KN
COUNT = COUNT + 1.0
IF(COUNT - 59.0)415,425,415
415 JFK = 1
KFJ = 5
416 WRITE OUTPUT TAPE 6,100,(R(K(KJ,NK),NK = JFK,KFJ)
COUNT = COUNT + 1.0
IF(COUNT - 59.0)417,426,417
417 JFK = KFJ + 1
KFJ = KFJ + 5
IF(KFJ - LAT)416,416,418
418 IF(KFJ - LAT - 5)419,420,419
419 KFJ = LAT
GO TO 416
420 IF(KN - IN)421,422,422
421 KN = KN + KK
GO TO 414
422 WRITE OUTPUT TAPE 6,307
COUNT = COUNT + 1.0
IF(COUNT - 59.0)422,423,208

```

EYE PROBLEM PROGRAMED BY LAWTON BLACKBURN JR.

```

423 WRITE OUTPUT TAPE 6,309,(CLASSF(I),I=1,3)
    NO = 1
    IF(SENSE SWITCH 4)424,156
424 WRITE OUTPUT TAPE 6,304,((RUNNO(I),I=1,3),(CLASSF(I),I=1,3)),IPAGE
    IPAGE = IPAGE + 1
    WRITE OUTPUT TAPE 6,232,(OMEGA(I),LEX(2*I-1),LEX(2*I),I = 1,10)
    WRITE OUTPUT TAPE 6,308,(CLASSF(I),I=1,3)
    GO TO 156
425 WRITE OUTPUT TAPE 6,309,(CLASSF(I),I=1,3)
    WRITE OUTPUT TAPE 6,304,((RUNNO(I),I=1,3),(CLASSF(I),I=1,3)),IPAGE
    IPAGE = IPAGE + 1
    COUNT=1.0
    GO TO 415
426 WRITE OUTPUT TAPE 6,309,(CLASSF(I),I=1,3)
    WRITE OUTPUT TAPE 6,304,((RUNNO(I),I=1,3),(CLASSF(I),I=1,3)),IPAGE
    IPAGE = IPAGE + 1
    COUNT=1.0
    GO TO 417
165 WRITE OUTPUT TAPE 7,104,T
    DO 168 KN=IM,IN,KK
    WRITE OUTPUT TAPE 7,106,KN
168 WRITE OUTPUT TAPE 7,100,(RIK(KN,NK),NK=1,LAT )
    GO TO 149
171 IF(SENSE SWITCH 2)170,9
170 PAUSE 77777
172 GO TO 9
174 FORMAT(14F5.3)
175 FORMAT(20I3)
176 FORMAT(7F10.8)
178 FORMAT(7F10.1)
180 FORMAT(18F4.1)
182 FORMAT(7F10.6)
    FORMAT(5F8.6,6I4)
184 FORMAT(2F4.3)
186 FORMAT(F9.2,F8.3,F9.0,F5.2,F6.3,F7.3,F6.3,5F4.3)
189 FORMAT(7F10.7)
190 FORMAT(5E14.5)
191 FORMAT(5E14.7)
192 FORMAT(30H END OF RELAXATION FOR TIME = F7.6)
194 FORMAT(1H 8H TIME = F9.7,8H      R = E12.5)
196 FORMAT(6H  I = I2)
198 FORMAT(5H      5F15.6)
200 FORMAT(////)
208 PAUSE 123456
    GO TO 27
217 IF(NO-NO1)149,165,149
218 IF(SENSE SWITCH 1)219,151
219 IF(NO-NO1)151,220,151
220 WRITE OUTPUT TAPE 7,102,T
    GO TO 151
413 WRITE OUTPUT TAPE 6,304,((RUNNO(I),I=1,3),(CLASSF(I),I=1,3)),IPAGE
    IPAGE = IPAGE + 1
    WRITE OUTPUT TAPE 6,200
224 WRITE OUTPUT TAPE 6,228,YIELD,ALT,DIST,FNUMB,ANGLE,FOCAL,AMUL,AMFL
    1,AMFH,RELHU,WMEI,CAF,PEI,CHOR,TEST,DELZ,DELW,NO1,IM,IN,KK,LONG,LAT
    2,DELT(1),DELT(2),DELT(3),DELT(4),DELT(5),DELT(6),DELT(7),DE

```

EYE PROBLEM PROGRAMED BY LAWTON BLACKBURN JR.

3LTI(8)

WRITE OUTPUT TAPE 6,200

WRITE OUTPUT TAPE 6,230,(FTIMS(I),I=1,8)

WRITE OUTPUT TAPE 6,305,(CLASSF(I),I=1,3)

SUM=0.0

GO TO 12

228 FORMAT( 9H YIELD = F9.2/9H ALT = F10.3/9H DIST = F10.0/9H FNUMR

1 = F10.2/9H ANGLE = F10.3/9H FOCAL = F10.5/9H AMIIL = F10.3/9H AMF

2L = F10.3/9H AMEH = F10.3/9H RELHU = F10.3/9H WMFI = F10.3/9H C

3AF = F10.3/9H RET = F10.6/9H CHOR = F10.6/9H TEST = F10.6/9H

4 DELZ = F10.6/9H DELP = F10.6/9H NO1 = I10/9H IM = I10/9H I

5N = I10/9H KK = I10/9H LONG = I10/9H LAT = I10/12H DELTI(

61) = F10.7/12H DELTI(2) = F10.7/12H DELTI(3) = F10.7/12H DELTI(4)

7 = F10.7/12H DELTI(5) = F10.7/12H DELTI(6) = F10.7/12H DELTI(7) = F

810.7/12H DELTI(8) = F10.7)

230 FORMAT(12H FTIMS(1) = F10.7/12H FTIMS(2) = F10.7/12H FTIMS(3) =

1F10.7/12H FTIMS(4) = F10.7/12H FTIMS(5) = F10.7/12H FTIMS(6) =

2F10.7/12H FTIMS(7) = F10.7/12H FTIMS(8) = F10.7)

232 FORMAT(23H OMEGA I J/(E12.5,3H I3,3H I3/))

300 FORMAT(3A6,3A6)

301 FORMAT(1H1 40X,3A6)

302 FORMAT(28X,3HSUM,26X,4HSUMD,25X,5HFTIME)

303 FORMAT(24X,E12.5,18X,F12.5,18X,E12.5)

304 FORMAT(1H1 10X,3A6,10X,3A6,21X,6H PAGE I4)

305 FORMAT(////////// 40X,3A6)

307 FORMAT(/)

308 FORMAT(//////////40X,3A6)

309 FORMAT(40X,3A6)

END(0,1,0,0,1,0,0,1,0,0,0,0,0,0,0)

END (0,1,0,1,1)

END FILE

\*N END TAPE

TABLE 3

PTRAN (atmospheric transmission less water vapor) (from 350 to 1500 microns in increments of 10 microns) ( $\times 10^3$ ).

551	589	623	656	685	712	746	758	776	795	812	827	839	852
863	874	882	891	898	906	913	918	923	929	934	938	941	945
949	952	955	957	959	962	964	966	968	969	970	972	974	976
977	978	979	980	981	981	982	983	984	984	985	986	987	988
988	989	989	990	990	990	991	991	992	992	992	993	993	993
994	994	994	994	995	995	995	995	995	995	995	996	996	996
996	996	996	996	996	996	997	997	997	997	997	997	997	997
997	997	998	998	998	998	998	998	998	998	998	998	998	998
998	998	998	998	998									

QTRAN (water vapor transmissivity) (from 350 to 1500 microns in increments of 10 microns) ( $\times 10^3$ ).

926	934	940	945	949	951	953	955	957	959	961	963	964	966
967	968	970	971	972	971	971	970	970	971	972	973	974	975
976	977	978	979	980	981	981	982	982	983	983	983	984	984
985	985	985	985	985	986	986	986	986	986	986	986	986	986
987	987	987	987	987	987	987	987	987	987	987	987	987	987
987	987	987	987	987	987	987	987	987	987	987	987	987	987
987	987	987	987	987	987	987	987	987	987	987	987	987	987
987	987	987	987	987	987	987	987	987	987	987	987	987	987
987	987	987	987	987	987	987	987	987	987	987	987	987	987
987	987	987	987	987	987	987	987	987	987	987	987	987	987

Absorption coefficient in ocular media  $\times 10^3$ . (ABSMO)

1000000	1000000	1000000	1000000	1000000	1000000	0900000
0620000	0575000	0500000	0425000	0333000	0285000	0240000
0223000	0185000	0160000	0130000	0115000	0100000	0090000
0075000	0060000	0050000	0037000	0033000	0033000	0033000
0033000	0033000	0033000	0033000	0033000	0033000	0033000
0033000	0033000	0033000	0033000	0033000	0033000	0033000
0033000	0033000	0033000	0033000	0033000	0033000	0033000
0033000	0033000	0033000	0033000	0033000	0033000	0033000
0033000	0033000	0033000	0033000	0033000	0033000	0033000
0060000	0075000	0088000	0110000	0150000	0200000	0250000
0534000	0575000	0582000	0582000	0582000	0550000	0525000
0475000	0400000	0300000	0250000	0210000	0200000	0210000
0225000	0260000	0290000	0360000	0410000	0680000	0810000
0880000	0900000	0920000	0930000	0940000	0950000	0940000
0930000	0920000	0910000	0905000	0900000	0905000	0910000
0920000	0940000	0970000	0980000	0985000	0990000	0993000
0995000	1000000	1000000	1000000	1000000	1000000	1000000
1000000	1000000	1000000	1000000	1000000		

TABLE 4

Reduced height,  $h_1$  and decimal percent, of the atmosphere for a station that is  $k$  km above sea level. (First three columns of this table from Kuiper, G.P., The Atmosphere of the Earth and Planets, 1952.)

$k$ (km)	$h_1$ (Winter) (km)	$h_1$ (Summer) (km)	Decimal Percent (Winter)	Decimal Percent (Summer)
0	8.03	8.05	1.00	1.00
1	7.09	7.15	0.884	0.890
2	6.26	6.34	0.780	0.787
3	5.51	5.61	0.686	0.697
4	4.83	4.95	0.602	0.615
5	4.23	4.36	0.526	0.541
6	3.68	3.82	0.458	0.475
7	3.20	3.34	0.399	0.415
8	2.76	2.91	0.344	0.361
9	2.38	2.53	0.296	0.314
10	2.04	2.18	0.254	0.281
12	1.45	1.61	0.180	0.200
14	1.09	1.19	0.136	0.128
16	0.79	0.88	0.098	0.011
18	0.58	0.65	0.072	0.081
20	0.42	0.48	0.053	0.060
25	0.19	0.22	0.024	0.027
30	0.09	0.11	0.011	0.014
35	0.04	0.05	0.005	0.006
40	0.02	0.02	0.003	0.003

The above table is used to find constants  $M_L$  and  $M_H$  (designated as AMFL and AMFH in program).

TABLE 5  
(Read Across)

Absorption coefficient in PE x 10<sup>3</sup>. (ABSI)

0853000	0825000	0805000	0775000	0750000	0730000	0723000
0717000	0714000	0712000	0710000	0700000	0687000	0675000
0665000	0650000	0625000	0600000	0575000	0550000	0530000
0505000	0480000	0457000	0435000	0420000	0400000	0385000
0370000	0355000	0343000	0333000	0315000	0300000	0287000
0273000	0260000	0250000	0240000	0225000	0215000	0205000
0195000	0187000	0180000	0175000	0168000	0162000	0157000
0152000	0150000	0145000	0140000	0137000	0130000	0125000
0120000	0120000	0120000	0120000	0120000	0120000	0120000
0120000	0120000	0120000	0120000	0120000	0120000	0120000
0120000	0120000	0120000	0120000	0120000	0120000	0120000
0120000	0120000	0120000	0120000	0110000	0110000	0110000
0110000	0110000	0120000	0125000	0134000	0140000	0145000
0140000	0137000	0135000	0127000	0120000	0110000	0107000
0102000	0100000	0100000	0113000	0125000	0140000	0150000
0160000	0175000	0190000	0200000	0215000	0230000	0350000
0510000	0675000	0840000	0975000			

Absorption coefficient in choroid x 10<sup>3</sup>. (ABSII)

0923000	0923000	0923000	0920000	0915000	0910000	0905000
0900000	0890000	0882000	0875000	0860000	0890000	0820000
0795000	0775000	0765000	0760000	0750000	0745000	0740000
0733000	0720000	0705000	0685000	0660000	0642000	0625000
0605000	0583000	0555000	0547000	0540000	0533000	0527000
0520000	0500000	0475000	0450000	0417000	0390000	0375000
0370000	0360000	0350000	0345000	0340000	0330000	0323000
0317000	0310000	0295000	0283000	0270000	0255000	0245000
0240000	0230000	0227000	0224000	0222000	0230000	0240000
0250000	0257000	0270000	0265000	0260000	0255000	0245000
0230000	0220000	0210000	0197000	0187000	0180000	0175000
0170000	0170000	0170000	0175000	0195000	0225000	0253000
0285000	0315000	0325000	0334000	0340000	0340000	0340000
0340000	0335000	0330000	0320000	0315000	0300000	0295000
0285000	0280000	0275000	0303000	0340000	0390000	0450000
0520000	0690000	0795000	0870000	0935000	0975000	0975000
0975000	0975000	0975000	0975000			

RUN G 4

UNCLASSIFIED

YIELD = 2.50  
 ALT = 0.  
 DIST = 1.  
 FNUMB = 8.50  
 ANGLE = 0.  
 FOCAL = 1.70000  
 AMUL = 1.000  
 AMFL = 1.000  
 AMFH = 0.  
 RELHU = 0.500  
 WMFI = 0.  
 CAF = 1.000  
 RET = 0.001000  
 CHOR = 0.010000  
 TEST = 0.010000  
 DELZ = 0.001000  
 DELR = 0.001000  
 NO1 = 1  
 IM = 1  
 IN = 49  
 KK = 3  
 LONG = 49  
 LAT = 25  
 DELT1(1) = 0.0000020  
 DELT1(2) = 0.0000200  
 DELT1(3) = 0.0002000  
 DELT1(4) = 0.0020000  
 DELT1(5) = 0.0200000  
 DELT1(6) = 0.2000000  
 DELT1(7) = -0.  
 DELT1(8) = -0.

FTIMS(1) = 0.0000100  
 FTIMS(2) = 0.0001000  
 FTIMS(3) = 0.0010000  
 FTIMS(4) = 0.0100000  
 FTIMS(5) = 0.1000000  
 FTIMS(6) = 0.5000000  
 FTIMS(7) = -0.  
 FTIMS(8) = -0.

TIME = 0.0000020 R = 0.78966E-02

I = 1	0.	0.	0.	0.	0.
	0.	0.	0.	0.	0.
	0.	0.	0.	0.	0.
	0.	0.	0.	0.	0.
	0.	0.	0.	0.	0.
I = 4	0.	0.	0.	0.	0.
	0.	0.	0.	0.	0.
	0.	0.	0.	0.	0.
	0.	0.	0.	0.	0.
	0.	0.	0.	0.	0.
	0.	0.	0.	0.	0.
I = 7	0.	0.	0.	0.	0.
	0.	0.	0.	0.	0.
	0.	0.	0.	0.	0.
	0.	0.	0.	0.	0.
	0.	0.	0.	0.	0.
	0.	0.	0.	0.	0.
I = 10	0.15304E-35	0.14907E-35	0.15205E-35	0.14445E-35	0.97883E-37
	0.14246E-35	0.82105E-37	0.14196E-35	0.33098E-37	0.
	0.	0.	0.	0.	0.
	0.	0.	0.	0.	0.
	0.	0.	0.	0.	0.
I = 13	0.70935E-28	0.69320E-28	0.70493E-28	0.67830E-28	0.34972E-29
	0.67053E-28	0.27577E-29	0.66837E-28	0.10394E-29	0.12683E-31
	0.78622E-34	0.69278E-36	0.22892E-38	0.	0.
	0.	0.	0.	0.	0.
	0.	0.	0.	0.	0.
I = 16	0.32881E-20	0.32369E-20	0.32675E-20	0.31785E-20	0.11227E-21
	0.31567E-20	0.77623E-22	0.31471E-20	0.24463E-22	0.34140E-24
	0.13466E-26	0.17209E-28	0.59825E-31	0.54929E-33	0.18024E-35
	0.13594E-37	0.	0.	0.	0.
	0.	0.	0.	0.	0.
I = 19	0.15237E-12	0.15055E-12	0.15143E-12	0.14931E-12	0.28225E-14
	0.14864E-12	0.11958E-14	0.14821E-12	0.76846E-15	0.11057E-16
	0.42292E-19	0.35648E-21	0.12240E-23	0.79536E-26	0.25851E-28
	0.14341E-30	0.45100E-33	0.22471E-35	0.69132E-38	0.
	0.	0.	0.	0.	0.
I = 22	0.70602E-05	0.70313E-05	0.70163E-05	0.69990E-05	0.55506E-07
	0.70003E-05	0.56322E-07	0.69803E-05	0.36193E-07	0.23683E-09
	0.87201E-12	0.39553E-14	0.13119E-16	0.51287E-19	0.16185E-21
	0.58383E-24	0.17899E-26	0.61405E-29	0.18477E-31	0.61248E-34
	0.18191E-36	0.	0.	0.	0.
I = 25	0.91084E 00	0.91084E 00	0.91085E 00	0.91085E 00	0.91085E 00
	0.91085E 00	0.91085E 00	0.90817E 00	0.23645E-02	0.62020E-05
	0.16363E-07	0.43379E-10	0.11545E-12	0.30831E-15	0.82567E-18
	0.22167E-20	0.59640E-23	0.16076E-25	0.43409E-28	0.11739E-30
	0.31787E-33	0.86180E-36	0.23385E-38	0.	0.
I = 28	0.57765E-01	0.57765E-01	0.57765E-01	0.57764E-01	0.57765E-01
	0.57765E-01	0.57765E-01	0.57595E-01	0.15034E-03	0.39536E-06

RUN G 4

0.10458E-08	0.27794E-11	0.74163E-14	0.19855E-16	0.53307E-19
0.14347E-21	0.38698E-24	0.10457E-26	0.28307E-29	0.76738E-32
0.20831E-34	0.56616E-37	0.	0.	0.
I = 31				
0.57766E-01	0.57766E-01	0.57766E-01	0.57766E-01	0.57766E-01
0.57766E-01	0.57765E-01	0.57595E-01	0.15034E-03	0.39535E-06
0.10457E-08	0.27793E-11	0.74157E-14	0.19853E-16	0.53300E-19
0.14345E-21	0.38690E-24	0.10455E-26	0.28298E-29	0.76710E-32
0.20822E-34	0.56588E-37	0.	0.	0.
I = 34				
0.57765E-01	0.57765E-01	0.57765E-01	0.57765E-01	0.57765E-01
0.57765E-01	0.57765E-01	0.57595E-01	0.14993E-03	0.39210E-06
0.10343E-08	0.27340E-11	0.72756E-14	0.19373E-16	0.51876E-19
0.13887E-21	0.37360E-24	0.10042E-26	0.27113E-29	0.73114E-32
0.19797E-34	0.53524E-37	0.	0.	0.
I = 37				
0.44661E-06	0.44661E-06	0.44661E-06	0.44661E-06	0.44661E-06
0.44661E-06	0.44659E-06	0.44268E-06	0.34328E-08	0.90023E-11
0.23747E-13	0.62881E-16	0.16748E-18	0.59482E-21	0.23922E-23
0.74764E-26	0.25915E-28	0.77469E-31	0.25175E-33	0.73628E-36
0.23092E-38	0.	0.	0.	0.
I = 40				
0.96400E-14	0.96402E-14	0.96402E-14	0.96402E-14	0.96402E-14
0.96402E-14	0.96389E-14	0.94729E-14	0.14627E-15	0.95552E-18
0.46929E-20	0.19944E-22	0.77670E-25	0.27901E-27	0.98857E-30
0.28261E-32	0.11873E-34	0.34997E-37	0.	0.
0.	0.	0.	0.	0.
I = 43				
0.20808E-21	0.20808E-21	0.20808E-21	0.20808E-21	0.20807E-21
0.20807E-21	0.20801E-21	0.20272E-21	0.46679E-23	0.40609E-25
0.24915E-27	0.12701E-29	0.57688E-32	0.24078E-34	0.94876E-37
0.	0.	0.	0.	0.
0.	0.	0.	0.	0.
I = 46				
0.44905E-29	0.44907E-29	0.44907E-29	0.44907E-29	0.44907E-29
0.44907E-29	0.44885E-29	0.43389E-29	0.13263E-30	0.16414E-32
0.13769E-34	0.92333E-37	0.	0.	0.
0.	0.	0.	0.	0.
0.	0.	0.	0.	0.
I = 49				
0.34900E-34	0.34902E-34	0.34902E-34	0.34902E-34	0.34902E-34
0.34902E-34	0.34880E-34	0.33539E-34	0.11907E-35	0.17042E-37
0.	0.	0.	0.	0.
0.	0.	0.	0.	0.
0.	0.	0.	0.	0.

UNCLASSIFIED

TIME = 0.0000300 R = 0.24619E-01

I = 1				
0.15589E-33	0.15540E-33	0.14631E-33	0.12610E-33	0.96962E-34
0.96530E-34	0.66356E-34	0.82898E-34	0.50409E-34	0.64494E-34
0.37374E-34	0.54505E-34	0.29132E-34	0.48003E-34	0.23054E-34
0.44211E-34	0.18429E-34	0.42713E-34	0.14397E-34	0.41690E-34
0.10443E-34	0.41069E-34	0.75889E-35	0.64515E-34	0.
I = 4				
0.21866E-30	0.21861E-30	0.20672E-30	0.17868E-30	0.13489E-30
0.13821E-30	0.89774E-31	0.11979E-30	0.67231E-31	0.93372E-31
0.49088E-31	0.79440E-31	0.37504E-31	0.70412E-31	0.28829E-31
0.65321E-31	0.22044E-31	0.63635E-31	0.15984E-31	0.62641E-31
0.99894E-32	0.62222E-31	0.76589E-32	0.94740E-31	0.94740E-31
I = 7				
0.11814E-25	0.11863E-25	0.11324E-25	0.98147E-26	0.71518E-26
0.77880E-26	0.45262E-26	0.68653E-26	0.32907E-26	0.53751E-26
0.23219E-26	0.46269E-26	0.16906E-26	0.41476E-26	0.12043E-26
0.38957E-26	0.80515E-27	0.38470E-26	0.43440E-27	0.38390E-26
0.43458E-27	0.38396E-26	0.47020E-27	0.54968E-26	0.54968E-26
I = 10				
0.64266E-21	0.64396E-21	0.62061E-21	0.54231E-21	0.37432E-21
0.44185E-21	0.21990E-21	0.39835E-21	0.15241E-21	0.31416E-21
0.10120E-21	0.27406E-21	0.66791E-22	0.24885E-21	0.39355E-22
0.23696E-21	0.26981E-22	0.23680E-21	0.26997E-22	0.23684E-21
0.27018E-22	0.23687E-21	0.28856E-22	0.31830E-21	0.31830E-21
I = 13				
0.34637E-16	0.34781E-16	0.33885E-16	0.29958E-16	0.19281E-16
0.25468E-16	0.10089E-16	0.23496E-16	0.63865E-17	0.18703E-16
0.37083E-17	0.16552E-16	0.18295E-17	0.15240E-16	0.17178E-17
0.14616E-16	0.16773E-17	0.14608E-16	0.16784E-17	0.14610E-16
0.16796E-17	0.14612E-16	0.17703E-17	0.18396E-16	0.18396E-16
I = 16				
0.18752E-11	0.18777E-11	0.18481E-11	0.16721E-11	0.96772E-12
0.14856E-11	0.41329E-12	0.14098E-11	0.21038E-12	0.11360E-11
0.12517E-12	0.10182E-11	0.11366E-12	0.93977E-12	0.10677E-12
0.90133E-12	0.10427E-12	0.90098E-12	0.10434E-12	0.90109E-12
0.10442E-12	0.90118E-12	0.10856E-12	0.10612E-11	0.10612E-11
I = 19				
0.10081E-06	0.10095E-06	0.10028E-06	0.93582E-07	0.46709E-07
0.88533E-07	0.12793E-07	0.86317E-07	0.10054E-07	0.70003E-07
0.85464E-08	0.62773E-07	0.72698E-08	0.57940E-07	0.66369E-08
0.55575E-07	0.64817E-08	0.55564E-07	0.64864E-08	0.55569E-07
0.64909E-08	0.55574E-07	0.66546E-08	0.61111E-07	0.61111E-07
I = 22				
0.53874E-02	0.53849E-02	0.53773E-02	0.52854E-02	0.51831E-02
0.52912E-02	0.51842E-02	0.52160E-02	0.42339E-02	0.42685E-02
0.41343E-02	0.38386E-02	0.36953E-02	0.35605E-02	0.33411E-02
0.34262E-02	0.33323E-02	0.34261E-02	0.33326E-02	0.34264E-02
0.33329E-02	0.34266E-02	0.33371E-02	0.35133E-02	0.35133E-02
I = 25				
0.67417E 01	0.67419E 01	0.67422E 01	0.67422E 01	0.67423E 01
0.67422E 01	0.67412E 01	0.67065E 01	0.58941E 01	0.58633E 01
0.58470E 01	0.54453E 01	0.54222E 01	0.51675E 01	0.50141E 01
0.50096E 01	0.50095E 01	0.50095E 01	0.50095E 01	0.50095E 01
0.50095E 01	0.50095E 01	0.50095E 01	0.50095E 01	0.50095E 01
I = 28				
0.44162E-00	0.44163E-00	0.44162E-00	0.44153E-00	0.44163E-00
0.44156E-00	0.44156E-00	0.43918E-00	0.38593E-00	0.38380E-00

RUN G 4

UNCLASSIFIED

0.38277E-00	0.35620E-00	0.35471E-00	0.33773E-00	0.32725E-00
0.32687E-00	0.32693E-00	0.32686E-00	0.32693E-00	0.32686E-00
0.32693E-00	0.32686E-00	0.32693E-00	0.32686E-00	0.32686E-00
I = 31				
0.44153E-00	0.44153E-00	0.44153E-00	0.44152E-00	0.44152E-00
0.44152E-00	0.44141E-00	0.43913E-00	0.38582E-00	0.38377E-00
0.38267E-00	0.35618E-00	0.35462E-00	0.33771E-00	0.32717E-00
0.32686E-00	0.32685E-00	0.32685E-00	0.32685E-00	0.32685E-00
0.32685E-00	0.32685E-00	0.32685E-00	0.32685E-00	0.32685E-00
I = 34				
0.44118E-00	0.44119E-00	0.44119E-00	0.44120E-00	0.44120E-00
0.44119E-00	0.44112E-00	0.43881E-00	0.38555E-00	0.38349E-00
0.38240E-00	0.35594E-00	0.35439E-00	0.33749E-00	0.32696E-00
0.32664E-00	0.32664E-00	0.32663E-00	0.32664E-00	0.32663E-00
0.32664E-00	0.32663E-00	0.32664E-00	0.32663E-00	0.32663E-00
I = 37				
0.34370E-03	0.34370E-03	0.34370E-03	0.34369E-03	0.34369E-03
0.34368E-03	0.34342E-03	0.33873E-03	0.28280E-03	0.27844E-03
0.27599E-03	0.25018E-03	0.24196E-03	0.22093E-03	0.21871E-03
0.21205E-03	0.21812E-03	0.21205E-03	0.21814E-03	0.21207E-03
0.21815E-03	0.21208E-03	0.21791E-03	0.20208E-03	0.20208E-03
I = 40				
0.64635E-08	0.64645E-08	0.64648E-08	0.64648E-08	0.64647E-08
0.64638E-08	0.64493E-08	0.62976E-08	0.53552E-08	0.52027E-08
0.51201E-08	0.46634E-08	0.42322E-08	0.94136E-09	0.35643E-08
0.41346E-09	0.35373E-08	0.41280E-09	0.35377E-08	0.41311E-09
0.35380E-08	0.41337E-09	0.35281E-08	0.25265E-09	0.25265E-09
I = 43				
0.12062E-12	0.12062E-12	0.12061E-12	0.12060E-12	0.12059E-12
0.12055E-12	0.12005E-12	0.11635E-12	0.10079E-12	0.96977E-13
0.94815E-13	0.86345E-13	0.74934E-13	0.24442E-13	0.59161E-13
0.15071E-13	0.57761E-13	0.94395E-14	0.57361E-13	0.66453E-14
0.57372E-13	0.66497E-14	0.57117E-13	0.40674E-14	0.40674E-14
I = 46				
0.22453E-17	0.22463E-17	0.22467E-17	0.22467E-17	0.22465E-17
0.22450E-17	0.22310E-17	0.21507E-17	0.18902E-17	0.18021E-17
0.17527E-17	0.15913E-17	0.13393E-17	0.55349E-18	0.10029E-17
0.38141E-18	0.96282E-18	0.28819E-18	0.94315E-18	0.19737E-18
0.93235E-18	0.10700E-18	0.92459E-18	0.65479E-19	0.65479E-19
I = 49				
0.16154E-20	0.16165E-20	0.16169E-20	0.16170E-20	0.16168E-20
0.16153E-20	0.16030E-20	0.15409E-20	0.13652E-20	0.12951E-20
0.12526E-20	0.11343E-20	0.93961E-21	0.43388E-21	0.68364E-21
0.31115E-21	0.64972E-21	0.24858E-21	0.63112E-21	0.18837E-21
0.61836E-21	0.12886E-21	0.60701E-21	0.42790E-22	0.

TIME = 0.0008900 R = 0.78037E-01

I = 1	0.25187E-12	0.24429E-12	0.23456E-12	0.22136E-12	0.20434E-12
	0.18407E-12	0.16183E-12	0.13920E-12	0.11765E-12	0.98242E-13
	0.81461E-13	0.67398E-13	0.55734E-13	0.46262E-13	0.38438E-13
	0.32252E-13	0.26958E-13	0.23051E-13	0.19221E-13	0.17191E-13
	0.14250E-13	0.15255E-13	0.14220E-13	0.26076E-13	0.
I = 4	0.55691E-11	0.54417E-11	0.52548E-11	0.49797E-11	0.46127E-11
	0.41674E-11	0.36724E-11	0.31645E-11	0.26785E-11	0.22405E-11
	0.18607E-11	0.15434E-11	0.12782E-11	0.10655E-11	0.88499E-12
	0.74970E-12	0.62173E-12	0.54608E-12	0.43819E-12	0.42438E-12
	0.30254E-12	0.40705E-12	0.31921E-12	0.77718E-12	0.77718E-12
I = 7	0.65116E-09	0.64692E-09	0.63185E-09	0.60346E-09	0.56256E-09
	0.51094E-09	0.45217E-09	0.39102E-09	0.33193E-09	0.27872E-09
	0.23214E-09	0.19386E-09	0.16056E-09	0.13586E-09	0.11132E-09
	0.98730E-10	0.76391E-10	0.78146E-10	0.47046E-10	0.74149E-10
	0.47880E-10	0.80763E-10	0.63883E-10	0.13771E-09	0.13771E-09
I = 10	0.72859E-07	0.71679E-07	0.69790E-07	0.66797E-07	0.62511E-07
	0.57006E-07	0.50648E-07	0.43974E-07	0.37463E-07	0.31689E-07
	0.26444E-07	0.22530E-07	0.18342E-07	0.16582E-07	0.12221E-07
	0.13706E-07	0.92612E-08	0.13516E-07	0.91956E-08	0.13538E-07
	0.93802E-08	0.14408E-07	0.11648E-07	0.21785E-07	0.21785E-07
I = 13	0.67820E-05	0.67603E-05	0.66527E-05	0.64309E-05	0.60770E-05
	0.55932E-05	0.50169E-05	0.44026E-05	0.37771E-05	0.32725E-05
	0.26910E-05	0.25033E-05	0.17532E-05	0.22375E-05	0.16536E-05
	0.21543E-05	0.16123E-05	0.21260E-05	0.16027E-05	0.21273E-05
	0.16223E-05	0.22116E-05	0.18663E-05	0.29360E-05	0.29360E-05
I = 16	0.53999E-03	0.53543E-03	0.52722E-03	0.51328E-03	0.49040E-03
	0.45654E-03	0.41579E-03	0.37418E-03	0.31915E-03	0.30890E-03
	0.25608E-03	0.28865E-03	0.24061E-03	0.27262E-03	0.22919E-03
	0.26307E-03	0.22411E-03	0.26015E-03	0.22308E-03	0.26009E-03
	0.22428E-03	0.26491E-03	0.24000E-03	0.30855E-03	0.30855E-03
I = 19	0.30352E-01	0.30348E-01	0.30125E-01	0.29695E-01	0.28944E-01
	0.27509E-01	0.25498E-01	0.25706E-01	0.23799E-01	0.23915E-01
	0.22244E-01	0.22419E-01	0.20892E-01	0.21160E-01	0.19895E-01
	0.20451E-01	0.19513E-01	0.20269E-01	0.19448E-01	0.20254E-01
	0.19470E-01	0.20347E-01	0.19828E-01	0.21319E-01	0.21319E-01
I = 22	0.93170E 00	0.93171E 00	0.92995E 00	0.92486E 00	0.92591E 00
	0.91924E 00	0.90679E 00	0.87894E 00	0.84459E 00	0.81447E 00
	0.79068E 00	0.76472E 00	0.74318E 00	0.72236E 00	0.70815E 00
	0.69955E 00	0.69674E 00	0.69491E 00	0.69514E 00	0.69442E 00
	0.69498E 00	0.69426E 00	0.69477E 00	0.69346E 00	0.69346E 00
I = 25	0.41601E 01	0.41624E 01	0.41585E 01	0.41582E 01	0.41495E 01
	0.41305E 01	0.40767E 01	0.39702E 01	0.38098E 01	0.36942E 01
	0.35977E 01	0.34942E 01	0.34041E 01	0.33210E 01	0.32582E 01
	0.32285E 01	0.32158E 01	0.32129E 01	0.32108E 01	0.32115E 01
	0.32105E 01	0.32116E 01	0.32119E 01	0.32136E 01	0.32136E 01
I = 28	0.79875E 00	0.79750E 00	0.79518E 00	0.79349E 00	0.79289E 00
	0.78870E 00	0.77800E 00	0.75658E 00	0.72724E 00	0.70320E 00

RUN G 4		UNCLASSIFIED		
0.68347E 00	0.66251E 00	0.64465E 00	0.62765E 00	0.61566E 00
0.60869E 00	0.60629E 00	0.60494E 00	0.60500E 00	0.60457E 00
0.60489E 00	0.60448E 00	0.60433E 00	0.60293E 00	0.60293E 00
I = 31				
0.50161E 00	0.50144E 00	0.50115E 00	0.50055E 00	0.49915E-00
0.49591E-00	0.48878E-00	0.47563E-00	0.45765E-00	0.44301E-00
0.43165E-00	0.41860E-00	0.40805E-00	0.39739E-00	0.39018E-00
0.38586E-00	0.38468E-00	0.38375E-00	0.38398E-00	0.38355E-00
0.38391E-00	0.38349E-00	0.38375E-00	0.38304E-00	0.38304E-00
I = 34				
0.42891E-00	0.42898E-00	0.42896E-00	0.42876E-00	0.42801E-00
0.42583E-00	0.42042E-00	0.40936E-00	0.39324E-00	0.38093E-00
0.37130E-00	0.36064E-00	0.35150E-00	0.34271E-00	0.33634E-00
0.33295E-00	0.33175E-00	0.33121E-00	0.33118E-00	0.33105E-00
0.33114E-00	0.33104E-00	0.33109E-00	0.33092E-00	0.33092E-00
I = 37				
0.66464E-01	0.66455E-01	0.66422E-01	0.66345E-01	0.66166E-01
0.65720E-01	0.64719E-01	0.62880E-01	0.60417E-01	0.58357E-01
0.56573E-01	0.54687E-01	0.52798E-01	0.51404E-01	0.50464E-01
0.49802E-01	0.49643E-01	0.49463E-01	0.49523E-01	0.49428E-01
0.49515E-01	0.49427E-01	0.49484E-01	0.49357E-01	0.49357E-01
I = 40				
0.20755E-02	0.20843E-02	0.20874E-02	0.20853E-02	0.20775E-02
0.20591E-02	0.20233E-02	0.19663E-02	0.18958E-02	0.18281E-02
0.17631E-02	0.16925E-02	0.16169E-02	0.15350E-02	0.14389E-02
0.13271E-02	0.13732E-02	0.13084E-02	0.13674E-02	0.13066E-02
0.13655E-02	0.12997E-02	0.13385E-02	0.12247E-02	0.12247E-02
I = 43				
0.36716E-04	0.36668E-04	0.36591E-04	0.36465E-04	0.36245E-04
0.35840E-04	0.35160E-04	0.34184E-04	0.33016E-04	0.31806E-04
0.30563E-04	0.29204E-04	0.27668E-04	0.25865E-04	0.23772E-04
0.21624E-04	0.19769E-04	0.17291E-04	0.17312E-04	0.14742E-04
0.17163E-04	0.14458E-04	0.16177E-04	0.12024E-04	0.12024E-04
I = 46				
0.46329E-06	0.46646E-06	0.46741E-06	0.46634E-06	0.46342E-06
0.45794E-06	0.44918E-06	0.43710E-06	0.42265E-06	0.40691E-06
0.38994E-06	0.37092E-06	0.34888E-06	0.32288E-06	0.29344E-06
0.26270E-06	0.23310E-06	0.20434E-06	0.18206E-06	0.15386E-06
0.14679E-06	0.10272E-06	0.12604E-06	0.75264E-07	0.75264E-07
I = 49				
0.26242E-07	0.26572E-07	0.26712E-07	0.26680E-07	0.26518E-07
0.26203E-07	0.25704E-07	0.25026E-07	0.24208E-07	0.23294E-07
0.22283E-07	0.21132E-07	0.19790E-07	0.18221E-07	0.16461E-07
0.14626E-07	0.12841E-07	0.11166E-07	0.97188E-08	0.83054E-08
0.73123E-08	0.57962E-08	0.52708E-08	0.27290E-08	0.

TIME = 0.0028900 R = 0.92437E-01

I = 1	0.11769E-05	0.11192E-05	0.10691E-05	0.10186E-05	0.96084E-06
	0.89472E-06	0.82152E-06	0.74352E-06	0.66340E-06	0.58383E-06
	0.50722E-06	0.43553E-06	0.37014E-06	0.31184E-06	0.26090E-06
	0.21716E-06	0.18019E-06	0.14947E-06	0.12438E-06	0.10483E-06
	0.89641E-07	0.81537E-07	0.73029E-07	0.84173E-07	0.
I = 4	0.50623E-05	0.48912E-05	0.47245E-05	0.45345E-05	0.43025E-05
	0.40289E-05	0.37209E-05	0.33890E-05	0.30447E-05	0.26999E-05
	0.23651E-05	0.20489E-05	0.17579E-05	0.14958E-05	0.12644E-05
	0.10635E-05	0.89145E-06	0.74732E-06	0.62469E-06	0.53695E-06
	0.43985E-06	0.45465E-06	0.40320E-06	0.62217E-06	0.62217E-06
I = 7	0.56059E-04	0.56179E-04	0.55478E-04	0.53867E-04	0.51550E-04
	0.48656E-04	0.45306E-04	0.41630E-04	0.37764E-04	0.33844E-04
	0.29991E-04	0.26309E-04	0.22877E-04	0.19743E-04	0.16933E-04
	0.14477E-04	0.12218E-04	0.10720E-04	0.80491E-05	0.98333E-05
	0.82571E-05	0.10701E-04	0.96980E-05	0.13367E-04	0.13367E-04
I = 10	0.64285E-03	0.62797E-03	0.61192E-03	0.59225E-03	0.56753E-03
	0.53780E-03	0.50377E-03	0.46645E-03	0.42707E-03	0.38685E-03
	0.34698E-03	0.30846E-03	0.27206E-03	0.23897E-03	0.20512E-03
	0.19050E-03	0.16726E-03	0.19054E-03	0.16690E-03	0.19241E-03
	0.17229E-03	0.20490E-03	0.19289E-03	0.23802E-03	0.23802E-03
I = 13	0.58879E-02	0.58852E-02	0.58230E-02	0.56929E-02	0.55064E-02
	0.52709E-02	0.49940E-02	0.46845E-02	0.43523E-02	0.40074E-02
	0.36596E-02	0.33312E-02	0.29047E-02	0.30517E-02	0.28068E-02
	0.29829E-02	0.27581E-02	0.29500E-02	0.27462E-02	0.29668E-02
	0.28029E-02	0.30844E-02	0.29953E-02	0.33592E-02	0.33592E-02
I = 16	0.51434E-01	0.50821E-01	0.50077E-01	0.49084E-01	0.47779E-01
	0.46153E-01	0.44230E-01	0.42053E-01	0.39677E-01	0.37564E-01
	0.36042E-01	0.36481E-01	0.34899E-01	0.35429E-01	0.34012E-01
	0.34719E-01	0.33497E-01	0.34384E-01	0.33350E-01	0.34447E-01
	0.33676E-01	0.35097E-01	0.34725E-01	0.36491E-01	0.36491E-01
I = 19	0.37176E-00	0.37126E-00	0.36907E-00	0.36479E-00	0.35853E-00
	0.35016E-00	0.33952E-00	0.33780E-00	0.33014E-00	0.32737E-00
	0.31929E-00	0.31680E-00	0.30948E-00	0.30818E-00	0.30236E-00
	0.30274E-00	0.29854E-00	0.30032E-00	0.29730E-00	0.30011E-00
	0.29811E-00	0.30195E-00	0.30112E-00	0.30593E-00	0.30593E-00
I = 22	0.22555E 01	0.22484E 01	0.22387E 01	0.22234E 01	0.22181E 01
	0.22105E 01	0.21889E 01	0.21641E 01	0.21285E 01	0.20981E 01
	0.20637E 01	0.20369E 01	0.20075E 01	0.19878E 01	0.19675E 01
	0.19585E 01	0.19483E 01	0.19472E 01	0.19424E 01	0.19447E 01
	0.19423E 01	0.19464E 01	0.19453E 01	0.19506E 01	0.19506E 01
I = 25	0.60548E 01	0.60728E 01	0.60838E 01	0.60871E 01	0.60794E 01
	0.60588E 01	0.60201E 01	0.59626E 01	0.58917E 01	0.58239E 01
	0.57607E 01	0.57010E 01	0.56473E 01	0.56016E 01	0.55662E 01
	0.55435E 01	0.55300E 01	0.55232E 01	0.55195E 01	0.55181E 01
	0.55172E 01	0.55174E 01	0.55174E 01	0.55182E 01	0.55182E 01
I = 28	0.21137E 01	0.21121E 01	0.21054E 01	0.20934E 01	0.20952E 01
	0.20856E 01	0.20722E 01	0.20470E 01	0.20211E 01	0.19902E 01

RUN G 4		UNCLASSIFIED		
0.19650E 01	0.19367E 01	0.19158E 01	0.18936E 01	0.18805E 01
0.18675E 01	0.18632E 01	0.18570E 01	0.18572E 01	0.18535E 01
0.18547E 01	0.18510E 01	0.18517E 01	0.18473E 01	0.18473E 01
I = 31				
0.11611E 01	0.11576E 01	0.11533E 01	0.11471E 01	0.11383E 01
0.11260E 01	0.11097E 01	0.10985E 01	0.10882E 01	0.10734E 01
0.10630E 01	0.10490E 01	0.10402E 01	0.10287E 01	0.10234E 01
0.10162E 01	0.10152E 01	0.10113E 01	0.10123E 01	0.10094E 01
0.10107E 01	0.10076E 01	0.10082E 01	0.10042E 01	0.10042E 01
I = 34				
0.82654E 00	0.82678E 00	0.82598E 00	0.82384E 00	0.82017E 00
0.81452E 00	0.80633E 00	0.79535E 00	0.78228E 00	0.76866E 00
0.76234E 00	0.75380E 00	0.74829E 00	0.74113E 00	0.73775E 00
0.73338E 00	0.73273E 00	0.73042E 00	0.73105E 00	0.72939E 00
0.73020E 00	0.72841E 00	0.72885E 00	0.72659E 00	0.72659E 00
I = 37				
0.22789E-00	0.22731E-00	0.22666E-00	0.22578E-00	0.22446E-00
0.22254E-00	0.21986E-00	0.21637E-00	0.21227E-00	0.20791E-00
0.20344E-00	0.19886E-00	0.19445E-00	0.19204E-00	0.19145E-00
0.18967E-00	0.18983E-00	0.18866E-00	0.18920E-00	0.18821E-00
0.18874E-00	0.18760E-00	0.18787E-00	0.18642E-00	0.18642E-00
I = 40				
0.35814E-01	0.35893E-01	0.35865E-01	0.35719E-01	0.35463E-01
0.35089E-01	0.34586E-01	0.33956E-01	0.33217E-01	0.32395E-01
0.31509E-01	0.30574E-01	0.29605E-01	0.28620E-01	0.27633E-01
0.26543E-01	0.26786E-01	0.26341E-01	0.26666E-01	0.26222E-01
0.26494E-01	0.25947E-01	0.26081E-01	0.25359E-01	0.25359E-01
I = 43				
0.49096E-02	0.48710E-02	0.48363E-02	0.47991E-02	0.47514E-02
0.46893E-02	0.46109E-02	0.45155E-02	0.44039E-02	0.42776E-02
0.41382E-02	0.39878E-02	0.38281E-02	0.36616E-02	0.34903E-02
0.33163E-02	0.31406E-02	0.29590E-02	0.28231E-02	0.27164E-02
0.28009E-02	0.26548E-02	0.26987E-02	0.25031E-02	0.25031E-02
I = 46				
0.56278E-03	0.56697E-03	0.56774E-03	0.56509E-03	0.55997E-03
0.55255E-03	0.54283E-03	0.53080E-03	0.51648E-03	0.49999E-03
0.48146E-03	0.46109E-03	0.43916E-03	0.41595E-03	0.39180E-03
0.36705E-03	0.34197E-03	0.31672E-03	0.29132E-03	0.26545E-03
0.24066E-03	0.20432E-03	0.21122E-03	0.18098E-03	0.18098E-03
I = 49				
0.16086E-03	0.16395E-03	0.16547E-03	0.16540E-03	0.16427E-03
0.16225E-03	0.15943E-03	0.15583E-03	0.15146E-03	0.14634E-03
0.14052E-03	0.13404E-03	0.12699E-03	0.11947E-03	0.11159E-03
0.10348E-03	0.95260E-04	0.87018E-04	0.78801E-04	0.70604E-04
0.62368E-04	0.53885E-04	0.45917E-04	0.34796E-04	0.

## BIBLIOGRAPHY

1. Geeraets, W.J., et al, "The Loss of Light Energy in Retina and Choroid", Archives of Ophthalmology, 64:606, 1960.
2. Armstrong, B.H., et al, Absorption Coefficients of Air from 22,000<sup>o</sup> to 220,000<sup>o</sup>, Headquarters AFSWC, Kirtland AFB, NMEX, SWC TR 58-36, 15 August 1958.
3. Brode, H.L., and R.E. Meyerott, Thermal Radiation from Atomic Detonations at Times Near Breakaway (U), The RAND Corporation, RM-1851, 7 August 1956, SECRET RESTRICTED DATA.
4. Brode, H.L., Close-in H-Bomb Effects (U), The RAND Corporation, RM-1583-1, Revised 3 February 1956, SECRET RESTRICTED DATA.
5. Brode, H.L., Point Source Explosion in Air, The RAND Corporation, RM-1824-AEC, 3 December 1956.
6. Brode, H.L., and F.R. Gilmore, Estimates of the Thermal Radiation from Nuclear Weapons Burst at High Altitudes (U), The RAND Corporation, RM-1983, 18 September 1957, SECRET RESTRICTED DATA.
7. Brode, H.L., Nuclear Blast Wave Calculations Including Thermal Losses (U), The RAND Corporation, RM-2076, 27 December 1957, SECRET.
8. Brode, H.L., Thermal Radiation from Nuclear Weapons (U), The RAND Corporation, S-82, 30 April 1958.
9. Brode, H.L., Theoretical Description of the Early Phases of the Fireball for a Very High Altitude Kiloton Explosion (U), The RAND Corporation, RM-2247, 2 September 1958, SECRET FORMERLY RESTRICTED DATA.
10. Brode, H.L., Theoretical Description of the Blast and Fireball for a Sea Level Megaton Explosion (U), The RAND Corporation, RM-2248, 2 September 1959, SECRET RESTRICTED DATA.
11. Lerohl, Major J.K., Retinal Burns from Nuclear Detonations (U), The RAND Corporation, RM-2424, 24 July 1959, SECRET RESTRICTED DATA.
12. Hillendahl, R.W., Characteristics of the Thermal Radiation from Nuclear Detonations, Vol III. U.S. Naval Radiological Defense Laboratory, AFSWP-902, 30 June 1959, SECRET RESTRICTED DATA.
13. Elswick, W.R., and H.H. Mitchell, M.D., An Evaluation of the Human Retinal Burn Problem Arising from Atomic Detonations, The RAND Corporation, RM-2500, 15 December 1959.

14. Meyerott, R.E., et al, Thermal Radiation Phenomena Associated with Nuclear Explosions in Air, Lockheed Missiles and Space Division, LMSD-703048, (DASA 1224), November 1960, SECRET RESTRICTED DATA.
15. Glasstone, S., ed., The Effects of Nuclear Weapons, Government Printing Office, 2nd Edition, to be published in April 1962.
16. Wray, J.L., Retinal Burn Problem Evaluation for High Altitude Nuclear Bursts (U), Headquarters Defense Atomic Support Agency, Washington 25, D.C., DASA 614, 1 July 1959, SECRET FORMERLY RESTRICTED DATA.
17. Kuiper, G.P., The Atmosphere of the Earth and Planets, 2nd ed., University of Chicago Press, Chicago, 1952.
18. List, R.J., compiler, Smithsonian Meteorological Tables, Smithsonian Institution, Washington, D.C., 1951.
19. Hoerlin, H.H., et al, High Altitude Explosions and Eyeburn Problem (U), Los Alamos Scientific Laboratory, LAMS 2337, August 14, 1959, SECRET RESTRICTED DATA.
20. Informal communicatio.. with Dr. W.J. Geeraets, Medical College of Virginia.
21. Carslwa, H.S., and J.C. Jaeger, Conduction of Heat in Solids, 2nd ed., Oxford, Clarendon Press, 1959.
22. Ham, W.T., Jr., "Flash Burns in the Rabbit Retina: As a Means of Evaluating the Retinal Hazard from Nuclear Weapons", American Journal of Opthamology, V. 46, No. 5, Pt 1, November 1958, pp. 700-723.
23. Richtmyer, F.K., et al, Introduction to Modern Physics, McGraw-Hill Book Company, Inc., New York, 1955.

DISTRIBUTION LIST

<u>ADDRESSEE</u>	<u>NO OF CYS</u>
<u>ARMY</u>	
Deputy Chief of Staff for Military Operations, D/A, Wash 25, D.C. ATTN: Dir of SW&R	1
Chief of Research & Development, D/A, Wash 25, D.C., ATTN: Atomic Div	1
Assistant Chief of Staff, Intelligence, D/A, Wash 25, D.C.	1
Chief Chemical Officer, D/A, Wash 25, D.C.	2
Chief of Engineers, D/A, Wash 25, D.C., ATTN: ENGNB	1
ATTN: ENGEB	1
ATTN: ENGTB	1
Office, Chief of Ordnance, D/A, Wash 25, D.C., ATTN: ORDTN	1
Chief Signal Officer, D/A, Plans, Programs & Operations Div., Wash 25, D.C., ATTN: SIGOP-7A	1
Chief of Transportation, D/A, Office of Planning & Intelligence, Wash 25, D.C.	1
The Surgeon General, D/A, Wash 25, D.C., ATTN: MEDNE	1
Commander-in-Chief, U.S. Army Europe, APO 403, New York, N.Y., ATTN: OPOT Div., Weapons Branch	1
Commanding General, U.S. Continental Army Command, Ft. Monroe, Va.	4
Director of Special Weapons Development Office, Hq CONARC, Ft. Bliss, Texas, ATTN: Captain Chester I. Peterson	1
President, U.S. Army Artillery Board, Ft. Sill, Okla.	1
President, U.S. Army Infantry Board, Ft. Benning, Ga.	1
President, U.S. Army Aviation Board, Ft. Rucker, Ala., ATTN: ATBG-DG	1
Commandant, U.S. Army Command & General Staff College, Ft. Leavenworth, Kan., ATTN: Archives	1
Commandant, U.S. Army Air Defense School, Ft. Bliss, Tex., ATTN: Command & Staff Dept	1
Commandant, U.S. Army Armored School, Ft. Knox, Ky.	1

<u>ADDRESSEE</u>	<u>NO OF CYS</u>
Commandant, U.S. Army Artillery & Missile School, Ft. Sill, Okla., ATTN: Combat Development Department	1
Commandant, U.S. Army Aviation School, Ft. Rucker, Ala.	1
Commandant, U.S. Army Infantry School, Ft. Benning, Ga., ATTN: C.D.S.	1
The Superintendent, U.S. Military Academy, West Point, N.Y., ATTN: Prof of Ordnance	1
Commandant, Quartermaster School, U.S. Army, Ft. Lee, Va., ATTN: Chief QM Library	1
Commandant, U.S. Army Ordnance School, Aberdeen Proving Ground, Md.	1
Commandant, U.S. Army Ordnance & Guided Missile School, Redstone Arsenal Ala.	1
Commanding General, Chemical Corps Training Command, Ft. McClellan, Ala.	1
Commandant, U.S. Army Signal School, Ft. Monmouth, N.J.	1
Commandant, U.S. Army Transportation School, Ft. Eustis, Va., ATTN: Security & Info Off	1
Commanding General, The Engineer Center, Ft. Belvoir, Va., ATTN: Asst CMDT, Engr School	1
Commanding General, Army Medical Service School, Brooke Army Medical Center, Ft. Sam Houston, Texas	1
Commanding Officer, 9th Hospital Center, APO 180, New York, N.Y., ATTN: CO U.S. Army Nuclear Medicine Research Detachment, Europe	1
Director, Armed Forces Institute of Pathology, Walter Reed Army Medical Center, Wash 25, D.C.	1
Commanding Officer, Army Medical Research Lab., Ft. Knox, Ky.	1
Commandant, Walter Reed Army Institute of Research, Walter Reed Army Medical Center, Wash 25, D.C.	1
Commanding General, QM R&D Command, QM R&D Center, Natick, Mass., ATTN: CBR Liaison Officer	1
Commanding General, U.S. Army Chemical Corps, Research & Development Command, Wash 25, D.C.	1
Commanding Officer, Chemical Warfare Lab., Army Chemical Center, Md., ATTN: Tech Library	1

<u>ADDRESSEE</u>	<u>NO OF CYS</u>
Commanding General, Engineer Research & Development Lab., Ft. Belvoir, Va., ATTN: Chief, Tech Support Branch	1
Director, Waterways Experiment Station, P.O. Box 631, Vicksburg, Miss., ATTN: Library	1
Commanding Officer, Diamond Ordnance Fuze Lab., Wash 25, D.C., ATTN: Chief, Nuclear Vulnerability Branch (230)	1
Commanding General, Aberdeen Proving Ground, Aberdeen Proving Ground, Md., ATTN: Ballistics Research Labs., ATTN: Dir, BRL	1
Commander, Army Ballistic Missile Agency, Redstone Arsenal, Ala., ATTN: ORDAB-HT	1
Commanding General, U.S. Army Electronic Proving Ground, Ft. Huachuca, Arizona, ATTN: Tech Library	1
Commanding Officer, USA Signal R&D Lab., Ft. Monmouth, N.J., ATTN: Tech Doc Center, Evans Area	1
Director, Operations Research Office, Johns Hopkins University, 6935 Arlington Rd., Bethesda 14, Md.	1
Commandant, U.S. Army Chemical Corps CBR Weapons School, Dugway Proving Ground, Dugway, Utah	1

NAVY

Chief of Naval Operations, D/N, Wash 25, D.C., ATTN: OPO3EG	1
ATTN: OP-75	1
ATTN: OP-91	1
ATTN: OP-922G1	1
ATTN: OP-922G2	1
Chief of Naval Personnel, D/N, Wash 25, D.C.	1
Chief of Naval Research, D/N, Wash 25, D.C., ATTN: Code 811	1
Chief, Bureau of Medicine & Surgery, D/N, Wash 25, D.C., ATTN: Special Wpns Def Div	1
Chief, Bureau of Ships, D/N, Wash 25, D.C., ATTN: Code 423	1
Chief, Bureau of Yards & Docks, D/N, Wash 25, D.C., ATTN: D-440	1
Director, U.S. Naval Research Lab., Wash 25, D.C., ATTN: Mrs. Katherine H. Cass	1
Commander, U.S. Naval Ordnance Lab., White Oak, Silver Spring, Md.	1

<u>ADDRESSEE</u>	<u>NO OF CYS</u>
Director, Material Laboratory, New York Naval Shipyard, Brooklyn 1, N.Y., ATTN: Mr. W. Dirksen and Mr. G. Mixter, M.D.	2
Commanding Officer & Director, Navy Electronic Lab., San Diego 52, Calif.	1
Commanding Officer, U.S. Naval Mine Defense Lab., Panama City, Fla.	1
Commanding Officer, U.S. Naval Radiological Defense Lab., San Francisco, 1 Calif., ATTN: Tech Info Div	1
Commanding Officer & Director, U.S. Naval Civil Engineering Lab., Port Hueneme, Calif., ATTN: Code L31	1
Commanding Officer, U.S. Naval Schools Command, U.S. Naval Station, Treasure Island, San Francisco, Calif.	1
Superintendent, U.S. Naval Postgraduate School, Monterey, Calif.	1
Officer-in-Charge, U.S. Naval School, CEC Officers, U.S. Naval Construction Battalion Center, Port Hueneme, Calif.	1
Commanding Officer, Nuclear Weapons Training Center, Atlantic, U.S. Naval Base, Norfolk 11, Va., ATTN: Nuclear Warfare Dept.	1
Commanding Officer, Nuclear Weapons Training Center, Pacific, Naval Station, San Diego, Calif.	1
Commanding Officer, U.S. Naval Damage Control Training Center, Naval Base, Philadelphia 12, Pa., ATTN: ABC Defense Course	1
Commanding Officer, Air Development Squadron 5, VX-5, Chana Lake, Calif.	1
Commanding Officer, Naval Air Material Center, Philadelphia 12, Pa., ATTN: Tech Data Branch	1
Commanding Officer, U.S. Naval Air Development Center, Johnsville, Pa., ATTN: NAS Librarian	1
Commanding Officer, U.S. Naval Medical Research Institute, National Naval Medical Center, Bethesda, Md.	1
Officer-in-Charge, U.S. Naval Supply Research & Development Facility, Naval Supply Center, Bayonne, New Jersey	1
Commandant, U.S. Marine Corps, Wash 25, D.C., ATTN: Code A03H	1
Director, Marine Corps Landing Force, Development Center, MCS, Quantico, Va.	1

<u>ADDRESSEE</u>	<u>NO OF CYS</u>
Commanding Officer, U.S. Naval CIC School, U.S. Naval Air Station, Glynco, Brunswick, Ga.	1
Chief of Naval Operation, D/N, Wash 25, D.C., ATTN: OP-09B5	1
Chief, Bureau of Naval Weapons, D/N, Wash 25, D.C., ATTN: RR12	1
<u>AIR FORCE</u>	
Hq USAF (AFCVC), ATTN: Operations Analysis Office, Wash 25, D.C.	1
Hq USAF (AFCIN-3), Wash 25, D.C.	1
Hq USAFE, APO 633, New York, N.Y.	1
Hq USAF (AFRDC), Wash 25, D.C.	1
Hq USAF (AFCSG), Wash 25, D.C.	1
TAC, Langley AFB, Va.	1
ADC, Ent AFB, Colo.	1
AFSC, Andrews AFB, Wash 25, D.C.	1
BSD, AF Unit Post Office, Los Angeles 45, Calif.	1
PACAF, APO 953, San Francisco, Calif.	1
AFRL, L.G. Hanscom Field, Bedford, Mass.	1
AFSWC, Kirtland AFB, New Mexico	1
AUL, Maxwell AFB, Ala.	1
Tech Tng Cen, Lowry AFB 30, Colo.	1
USAF Aerospace Med Cent, ATTN: Lt Col Ralph Allen, Brooks AFB, Texas	1
1035th USAF Fld Acty Gp, Wash 25, D.C.	1
ASD, ATTN: Aerospace Medical Laboratory (MRVPV), FOR: Capt. L.R. Loper, Wright-Patterson AFB, Ohio	1
Director, USAF Project RAND, via: Air Force Liaison Office, The RAND Corporation, 1700 Main Street, Santa Monica, Calif.	1
RADC, Griffiss AFB, N.Y.	1
FTD, Wright-Patterson AFB, Ohio	1

ADDRESSEENO OF CYSOTHER AGENCIES

Director of Defense Research & Engineering, Wash 25, D.C., ATTN: Tech Library	1
Director, Weapons Systems Evaluation Group, Room 1E880, the Pentagon, Wash 25, D.C.	1
U.S. Documents Officer, Office of the United States National Military Representative - SHAPE, APO 55, New York, N.Y.	1
Chief, Defense Atomic Support Agency, Wash 25, D.C.	10
Commander, Field Command, DASA, Sandia Base, Albuquerque, New Mexico ATTN: FCTG	1
Commander, Field Command, DASA, Sandia Base, Albuquerque, New Mexico	16
Administrator, National Aeronautics & Space Administration, 1520 "H" St., N.W., Wash 25, D.C., ATTN: Mr. R.V. Rhode	1
SAC (OAWS), Offutt AFB, Nebr	1
Commandant, US Coast Guard, 1300 E. Street, N.W., Wash 25, D.C., ATTN: (OIN)	1
ASTIA, Arlington Hall Station, Arlington 12, Va.	15
Los Alamos Scientific Lab., P.O. Box 1663, Los Alamos, New Mexico, Report Librarian	1
Chief, Classified Technical Library, Technical Library, Technical Information Service, USAEC, Wash 25, D.C., ATTN: Mrs. Jean O'Leary	1
Medical College of Virginia, Department of Surgery, 12th & Broad Sts., Richmond 19, Va., FOR: Dr. William T. Ham	2
Los Alamos Scientific Lab., P.O. Box 1663, Los Alamos, New Mexico, New Mexico, FOR: Dr. Herman Hoerlin (J10)	1
Mr. Laurence S. Cohan, OEG Representative, c/o Staff, Commander, Anti-Submarine Forces, Atlantic, U.S. Atlantic Fleet, U.S. Naval Base, Norfolk 11, Virginia	1